NASI. 26: 3006

JUN 29 1978

NASA Contractor Report 3006

COMPLETED

ORIGINAL

Horizontal Eddy Diffusivities in the Northern Hemispheric Stratosphere and Lower Mesosphere

S. K. Kao, R. J. Okrasinski,
and N. J. Lordi

CONTRACT NAS6-2498
JUNE 1978

NASA

75

NAS1.26:3006

NASA Contractor Report 3006

Horizontal Eddy Diffusivities in the Northern Hemispheric Stratosphere and Lower Mesosphere

S. K. Kao, R. J. Okrasinski,
and N. J. Lordi
University of Utah
Salt Lake City, Utah

Prepared for
Wallops Flight Center
under Contract NAS6-2498

NASA
National Aeronautics
and Space Administration

Scientific and Technical
Information Office

1978

HORIZONTAL EDDY DIFFUSIVITIES IN THE NORTHERN HEMISPHERIC STRATOSPHERE AND LOWER MESOSPHERE

by

S. K. Kao, R. J. Okrasinski and N. J. Lordi

University of Utah

SUMMARY

Meteorological rocket soundings, launched between 1969-74 at six locations representative of low, middle, and high altitudes, are employed with the use of the statistical theory of diffusion, to determine the zonal and meridional component of eddy diffusivity between 30 and 55 km as a function of season, latitude, and altitude. A comparison is also made between annually-averaged eddy diffusivities above and below 30 km.

It is shown that the zonal component of eddy diffusivity is approximately three to five times as large as the meridional component, in most cases. Both components of eddy diffusivity vary greatly with season, latitude, and altitude. Highest eddy diffusivities, found in the vicinity of the winter westerly jet, are approximately one order of magnitude higher than those present during the summer. Tropical eddy diffusivities, however, remain relatively small throughout the year. Annually, a minimum is indicated near 25 km between maximums located at the stratopause and tropopause.

INTRODUCTION

In recent years, the turbulent transport processes in the stratosphere have been of great interest due to the possible deleterious effects of SST travel and chloro-fluoro-methanes upon the ozone layer. Most research efforts have been directed toward construction of diffusion models with the use of assumed eddy diffusivity. Reed and German (1965), for example, suggested the following equation:

$$\frac{\partial \bar{c}}{\partial t} = K_Y \frac{\partial^2 \bar{c}}{\partial Y^2} + K_Z \frac{\partial^2 \bar{c}}{\partial Z^2} + \Gamma K_Z \frac{\partial \bar{c}}{\partial Z}$$

where X, Y, and Z are coordinates in the principal axis system, K_Y and K_Z are eddy diffusivities, c is the concentration, and $\Gamma = \rho^{-1} \frac{\partial \rho}{\partial Z}$. Approximate K_Y and K_Z are determined by

$$K_Y = K_{yy}$$

$$K_Z = \overline{\alpha'^2} K_{yy} ,$$

where K_{yy} is the meridional component of eddy diffusivity, and α is the slope of the mixing path. Because of the lack of measured values of the eddy diffusivity in the upper atmosphere, earlier investigations used exclusively estimated values of eddy diffusivity, which vary greatly, especially above the radiosonde level; therefore, the computed concentration distributions in the upper atmosphere vary widely, and little confidence can be placed in their results. Values of $\overline{\alpha'^2}$ cannot be readily determined since there are no measurements of the slope of isentropic surfaces above 30 km. However, in a future study $\overline{\alpha'^2}$ will be estimated.

The aim of this study is to determine the zonal and meridional components of eddy diffusivity in the upper stratosphere and lower mesosphere as a function of season, latitude, and altitude. This is accomplished by statistical analysis of the zonal and meridional components

of wind velocity measured between 28 and 57 km by meteorological rockets launched between 1969-74 at various latitudes. Annual eddy diffusivities are also calculated and compared with eddy diffusivities below 30 km.

THEORETICAL BACKGROUND

Statistical theory, first formulated by G. I. Taylor (1921), is used to determine the zonal and meridional components of eddy diffusivity. The turbulent component of wind velocity in the ith direction, $u_i(t)$, is assumed to be statistically stationary in which case the autocorrelation function

$$R_i(\tau) = \frac{[u_i(t)\ u_i(t+\tau)]}{[u_i^2(t)]}, \qquad (1)$$

where

$$R_i(\tau) \to 1 \text{ as } \tau \to 0 ,$$

$$R_i(\tau) \to 0 \text{ as } \tau \to \infty ,$$

is both stationary and even. If the autocorrelation function is integrated between 0 and some lag t_L, where $R(t_L)$ approaches 0, the resulting quantity is known as the integral time scale

$$I_i = \int_0^{t_L} R_i(\tau)d\tau .$$

Taylor (1921) demonstrated that the rate of change of the square of particle distance can be expressed as

$$\varepsilon_i = \frac{1}{2}\, d\, \frac{[x_i^2(t)]}{dt} = \frac{1}{2}\left[\frac{d(x_i^2(t))}{dt}\right] = [x_i(t)\ \frac{d\ x_i(t)}{dt}]$$

$$= [x_i(t)\ u_{Li}(t)],$$

where U_{Li} is the Lagrangian wind velocity, or the velocity of a fluid particle. Since

$$x_i(t) = \int_0^t u_{Li}(t')dt' \ ,$$

$$\frac{1}{2} d \frac{[x_i^2(t)]}{dt} = \int_0^t [u_{Li}(t)\ u_{Li}(t')]dt'.$$

Integrating both sides with respect to t and letting $t'=t-\tau$

$$\frac{1}{2} [x_i^2(t)] = \int_0^t \int_0^{t'} [u_{Li}(t'-\tau)\ u_{Li}(t')]d\tau\ dt'.$$

Substituting (1) remembering that $R_i(\tau) = R_i(-\tau)$

$$[x_i^2(t)] = 2[u_i^2(t)] \int_0^t \int_0^{t'} R_{Li}(\tau)\ d\tau\ dt'.$$

Thus the ith component of eddy diffusivity can be expressed as

$$\varepsilon_i(t) = [u_i^2(t)] \int_0^t R_{Li}(\tau)\ d\tau,$$

which for large diffusion time t becomes

$$\varepsilon_i(t) = [u_i^2(t)]\ \ I_{Li} = K_{ii}.$$

In the atmosphere, however, Eulerian wind velocities, observed at a fixed location, are more frequently measured. Hay and Pasquill (1959) assumed that the Eulerian autocorrelation function could be related to the Lagrangian autocorrelation function by

$$R_{Ei}(\tau) = R_{Li}(B_i\tau)$$

where

B_i is a constant.

Integrating both sides from 0 to infinity

$$\int_0^\infty R_{Ei}(\tau)\, d\tau = \int_0^\infty R_{Li}\,(B_i\tau)\, d\,(B_i\tau)$$

$$= \frac{1}{B_i} \int_0^\infty R_{Li}(\tau)\, d\tau,$$

so that

$$B_i I_{Ei} = I_{Li}.$$

We can, therefore, determine the zonal and meridional components of eddy diffusivity by

$$K_{xx} = [u^2(t)]\, B_u\, I_{Eu} \tag{2}$$

$$K_{yy} = [v^2(t)]\, B_v\, I_{Ev} \tag{3}$$

For the case of large-scale turbulence, Kao and Bullock (1964) and Murgatroyd (1969) have found B_i to be between .3 and .6 for heights ranging up to the lower stratosphere. However, since upper stratospheric and mesospheric dynamics are inherently different from tropospheric motions, it would be expected that B_i values should differ. In this study B_i values were found using the following relationship (Kao, 1965):

$$B_i = \left|\frac{C}{\bar{u}-C}\right|, \tag{4}$$

where C represents the phase speed of the dominant wave at a particular altitude and $\bar{u}$ is the value of the mean zonal wind.

For the winter and fall seasons, values of C at levels up to 55 km were obtained with the use of joint NASA and NOAA high atmosphere synoptic analyses for 1972 (NASA SP-3091, 1975). Due to the relative flatness of

pressure patterns in the spring and summer the above synoptic analyses could not be used; however, Muench (1968) analyzed summertime balloon ascents in order to determine the existence of a dominant 12 day traveling planetary wave for latitudes from 20 - 50°N ranging between 25 - 45 km. This information, together with a knowledge of the mean zonal winds, yield a B_i of about 1/3 for both stratosphere and lower mesosphere. The wintertime stratosphere is dominated by vertically propagating quasi-stationary waves leading to very small phase speed and hence small B_i. Using phase speeds determined from the upper atmospheric synoptic analyses, it was determined that B_i ranged between .56 at 30 km and .12 at 55 km in winter and between .33 at 30 km and .08 at 55 km in fall. Values used in this study are given in Table 35.

METHODS OF COMPUTATION

Rocketsonde Data

Zonal and meridional wind velocities, in one kilometer increments between 28 and 57 km, were obtained from rocketsondes launched between 1969-74 in the Western Meridional Network. NASA Wallops Island, Virginia, supplied the necessary data. Although rocketsonde launchings are often scheduled every two of three days, there are occasionally much larger gaps between observations. On the other hand, some launchings are one day apart or less. In order to analyze latitudinal cross-sections of the Northern Hemisphere, the following ten stations were selected:

1. Poker Flats, Alaska (65°N, 148°W)
2. Ft. Greely, Alaska (64°N, 146°W)
3. Ft. Churchill, Canada (59°N, 94°W)
4. Wallops Island, Virginia (38°N, 75°W)
5. Pt. Mugu, California (34°N, 119°W)
6. White Sands, New Mexico (32°N, 106°W)
7. Cape Kennedy, Florida (28°N, 81°W)
8. Barking Sands, Hawaii (22°N, 160°W)
9. Ft. Sherman, Panama (9°N, 80°W)
10. Kwajalein, Marshall Islands (9°N, 168°W)

Because of large gaps existing at some of the above locations, the following stations close in latitude were combined:

1. Ft. Greely, Poker Flats, Ft. Churchill
2. Pt. Mugu, White Sands
3. Kwajalein, Ft. Sherman

Wind velocities were, therefore, available for six latitudes.

The sparsity of the rocket network prevented any consideration of longitudinal variations. It should also be noted that eight of the ten stations are located in North America so that during the winter and fall the quantities computed and illustrated in this study are more representative of that continent than they are of the Northern Hemisphere in general. During spring and summer, the flow is almost symmetric around the pole due to the trapping of vertically propagating planetary waves by the mean easterly flow (Charney and Drazin, 1961).

For the purposes of this study, the data were divided into the following four seasons: winter (January-March); spring (April-June); summer (July-September); and fall (October-December). For each six-year period, the number of launch days available in each season ranged from 110 - 160 at Wallops Island to 290 at some of the combined locations.

Since most rocketsondes are launched near local noon, fluctuations due to the diurnal oscillation were easily avoided. First, for each station, all soundings launched several hours outside of the estimated mean launch time were visually edited. For each altitude, all rocketsonde data from the same day were then averaged. Finally, for each year, season, and station a mean launch time was calculated, and all data not acquired within three hours of this quantity were rejected.

Instrument errors in the above data were reduced by performing a three point vertical smoothing at 55, 50, 45, 40, 35, and 30 km. Next, gross errors were eliminated by removing a linear trend for each year, season, station, and altitude, and then rejecting all velocities greater than 2.3 multiplied by the standard deviation. Finally, from the edited data, the mean zonal and meridional wind velocities were calculated and linear trends were again removed, in order to obtain the turbulent fluctuations necessary to compute the variances and autocorrelations.

Since six-year autocorrelation functions were desired,

$$R_u(\tau) = \left(\sum_{i=1}^{N(\tau)} u_i(t)\, u_i(t+\tau) \right) / (N(\tau)\sigma_u^2)$$

$$R_v(\tau) = \left(\sum_{i=1}^{N(\tau)} v_i(t)\, v_i(t+\tau) \right) / (N(\tau)\sigma_v^2)$$

were calculated for each season, station, and latitude; where u(t) and v(t) are the zonal and meridional wind perturbations, τ is the lag time, $N(\tau)$ is the total number of soundings, τ days apart, during the six-year period, and σ_u^2 and σ_v^2 are the total six-year zonal and meridional variances. $R_u(0)$ and $R_v(0)$ were assumed to be 1. In this manner, years with more wind measurements were given more weight in the calculations. Although autocorrelations were calculated for all lags between 1 and 40 days whenever $N(\tau)$ was greater than 34, most values of $N(\tau)$ ranged between 80 - 140 for τ less than 10 days.

The Eulerian integral time scales were obtained by integrating the autocorrelation functions with respect to τ. After linear regressions with altitude were computed at each station, the smoothed integral time scales were multiplied by the variances and the Lagrangian transformation B_i, in order to obtain the zonal and meridional components of eddy diffusivity.

Six-year seasonal means, variances, Eulerian integral time scales and eddy diffusivities in the zonal and meridional direction are tabulated in Tables 1-35 and analyzed in Figures 1-34.

Radiosonde Data

For the sake of comparison, it was desirable to calculate some eddy diffusivities for the troposphere and lower stratosphere. Integral

time scales were readily available from Kao and Gain (1968) and Kao and Powell (1969), who computed the annual Lagrangian autocorrelation functions from the surface to 32 km at 47°N. Fortunately, the integral time scales vary with latitude much less than the variances. The latter, computed from standard deviations calculated from radiosondes launched between July 1957 - December 1964, and tabulated by Newell and others (1972), were available in 10° increments between 0°N and 70°N.

Eddy diffusivities, calculated with this data, were then combined with the annual mean diffusivities previously computed above 30 km, to obtain the latitudinal cross sections shown in Figures 33 and 34.

DISCUSSION OF THE RESULTS

E-W Mean

The dominance of the westerlies, between August and April, and the easterlies, during the spring and summer, are clearly shown in Figures 1-4. Maximum easterly winds are somewhat weaker and are located at a lower latitude than the maximum winter westerlies. In Figures 1 and 4, some indication of the semi-annual oscillation is seen near the equatorial stratopause, where the annual wave amplitude is close to zero according to Belmont et al. (1973).

N-S Mean

As shown in Figures 5-8, the meridional component of mean wind velocity is approximately one-fifth as strong as the zonal wind. Again, a seasonal variation exists, with weaker winds in evidence during the spring and summer. Both seasons are characterized both by two weak maximums of southerly flow located in the lower mesosphere near 45°N and 20°N and extremely weak flow below 45 km. In contrast, winter and fall are dominated by relatively strong northerlies in the middle stratospheric polar regions and strong southerly flow in the lower mesospheric middle latitudes.

E-W Variance

Zonal variances are analyzed in Figures 9-12, in order to obtain some estimate of the average zonal eddy intensity. A much more marked seasonal, latitudinal, and altitudinal dependence is evident, with an order of magnitude difference separating the variances in the middle and high latitude westerlies from those in the summer easterlies. Below 25°N, however, the difference between winter and spring diminishes with decreasing latitude until no seasonal variation is evident south of 10°N. The lowest variances are also found in this region, generally below 35 km. Spring and summer are characterized by both an absence of latitudinal variation and a positive correlation of variance with altitude. In contrast, winter and fall are marked by large latitudinal changes; with maximum variances located in the vicinity of the winter westerly jet. The fall latitude-height section differs somewhat from the winter illustration, however, due to the lower variances evident below 45 km and to the presence of a second strong maximum near the subtropical stratopause.

N-S Variance

Latitudinal cross sections of the meridional variances are analyzed in Figures 13-16. Although less than one-half the magnitude of the zonal variances, they change similarly with season, latitude, and altitude. A lack of seasonal variation is again indicated for the tropical regions; while the more northern latitudes are characterized by an order of magnitude difference between summer and winter. Variances in the middle stratospheric equatorial regions are again small. During spring and summer, a gradual increase with altitude is also characteristic of the meridional variances. Large latitudinal variations are again indicated for winter and fall, but, in the latter season, the maximum is located in the polar mesosphere instead of at the mid-latitude stratopause.

E-W Integral Time Scale

The zonal Eulerian integral time scales, illustrated by Figures 17-20, exhibit a much smaller variation with season, latitude, and altitude than the variances. In the tropics, both a lack of seasonal

variability and short integral time scales are characteristic. The longest time scales in the middle and high latitudes are present during the summer and fall when they are approximately twice as long as those found during the rest of the year. Maximums are located in the mid-latitude stratosphere during the winter, spring, and summer; at the mid-latitude stratopause in summer and fall; and above 45 km in the subtropics during winter and fall.

N-S Integral Time Scale

The meridional Eulerian integral time scales, illustrated in Figures 21-24, are apparently only one-third to one-fifth as long as their zonal counterparts. Again, the shortest time scales are found near the equator and, again, seasonal variation is lacking in this region. In this case, however, the longest integral time scales occur during the winter and fall. Maximums are evident in the middle latitudes below 45 km, during the summer, fall, and winter; in the subtropics above 50 km, in the spring, summer, and fall; and in the polar middle stratosphere during spring.

E-W Eddy Diffusivity

A strong seasonal, latitudinal, and altitudinal variation of the zonal component of eddy diffusivity is apparent in Figures 25-28. The smallest diffusion rates occur in the equatorial regions, where a lack of seasonal variation is evident. Seasonally, in the more northern latitudes, the smallest eddy diffusivities occur during the spring, with somewhat higher diffusion rates expected in the summer, and much more rapid diffusion indicated for the fall and winter. Two strong diffusivity maxima are characteristic of the latter two seasons, as well as strong diffusivity gradients for these seasons between 20°N and 30°N at all levels. The strong wintertime maximum occurs around 38°N at 35 km, while separate fall maxima are evident around 30°N at about 33 km and 50 km. Much weaker gradients prevail in spring and summer at most levels; however, a noticeable increase in eddy diffusivity in summer occurs above

40 km at 50°N. The prevailing factor in the determination of the wintertime eddy diffusivity maximum appears to be the general increase in the variance in this region.

N-S Eddy Diffusivity

Many similarities between the latitude-altitude sections of the meridional component of eddy diffusivity analyzed in Figures 29-32 and the four previous illustrations are obvious. Again, both an order of magnitude difference between the diffusivities in the summer easterlies and winter westerlies and a lack of seasonal variability south of 10°N are evident. Altitude and, during the winter and fall, latitude are again important. Summer and spring analyses are similar in distribution and magnitude, with maximum eddy diffusivities occurring above the stratopause. The winter maximum again occurs around 35 km at 40°N, and a strong wintertime diffusivity gradient is apparent between 30°N and 40°N at levels up to 50 km. Fall diffusivities are relatively small below 50°N; however, north of 50°N values increase reaching maximum around 60°N between 30 and 35 km. It may be noticed that in all cases the meridional component of diffusivity is substantially less than its zonal counterpart. The winter meridional maximum is about one-quarter the zonal maximum, while the summer maximum is an order of magnitude less than its zonal counterpart.

Annual Eddy Diffusivity

The variation with altitude and latitude of the mean annual zonal and meridional components of eddy diffusivity is seen in Figures 33 and 34. Obviously, these illustrations can be discussed simultaneously since the only major differences are the more northerly positioning of the meridional maximum and the greater diffusion rates evident in the zonal direction. With respect to the zonal eddy diffusivity component, there is a tropopausal maximum at 40°N and a maximum of equal magnitude at 40°N at a level of 35 km. Tropical values are 10-20 percent of the mid-latitude values. The meridional component maximum in the troposphere is about one-half its zonal value, while the stratospheric maximum is about

one-third its zonal value. The meridional stratospheric maximum shifts northward to 60°N, while stratospheric values of this component are very small south of 40°N.

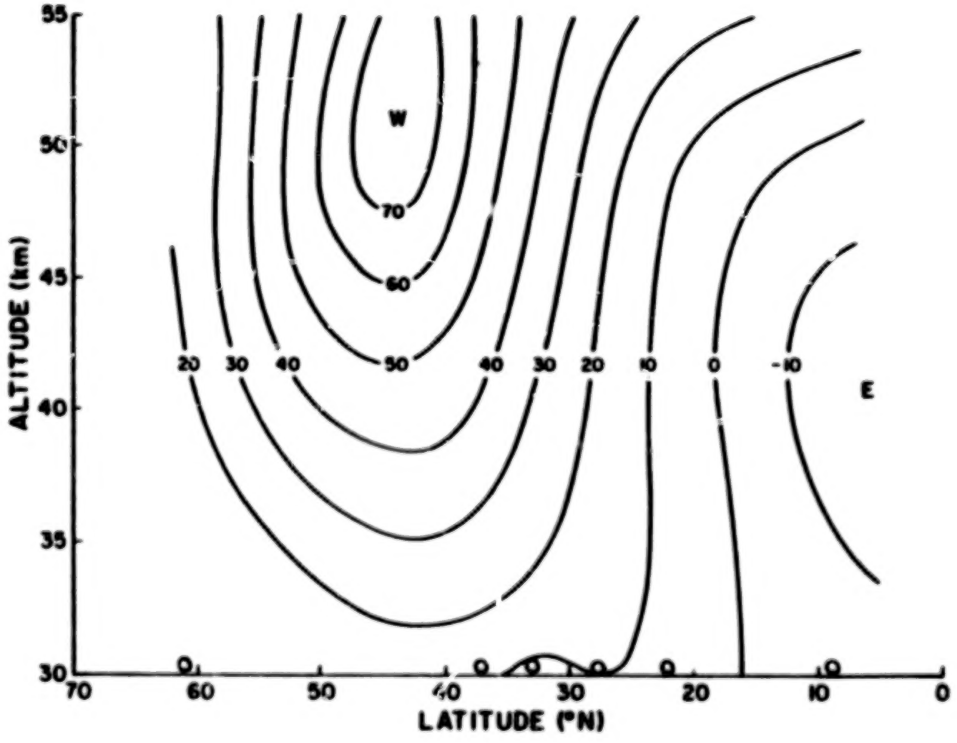

Fig. 1. Latitude-height section of the mean zonal wind (m sec^{-1}), Winter 1969-1974

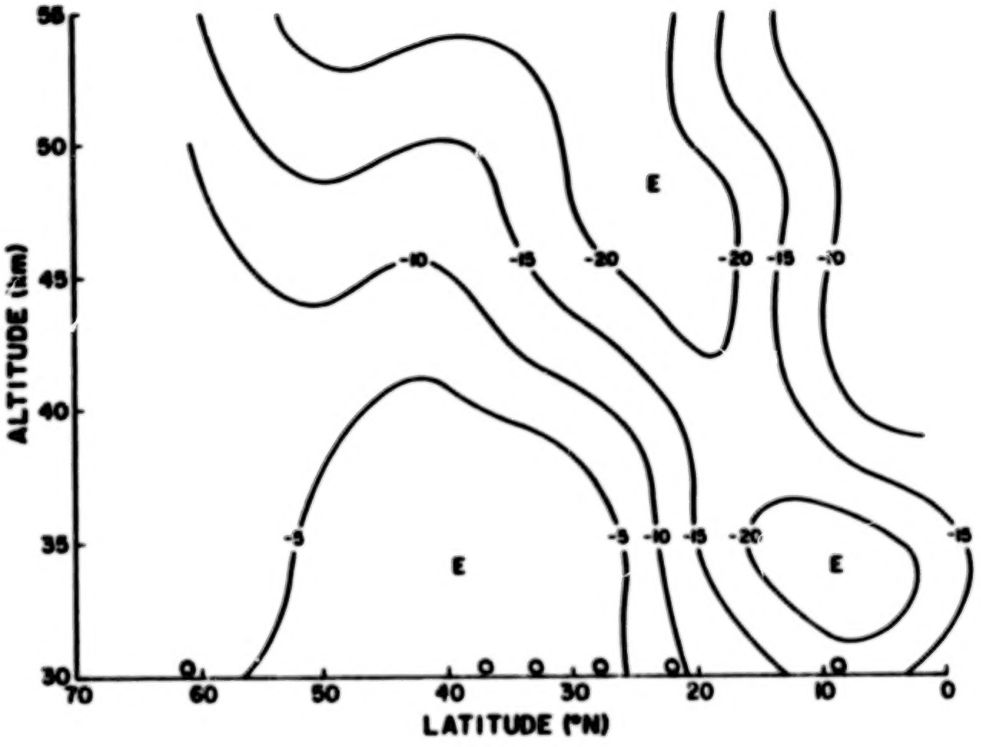

Fig. 2. Latitude-height section of the mean zonal wind (m sec^{-1}), Spring 1969-1974.

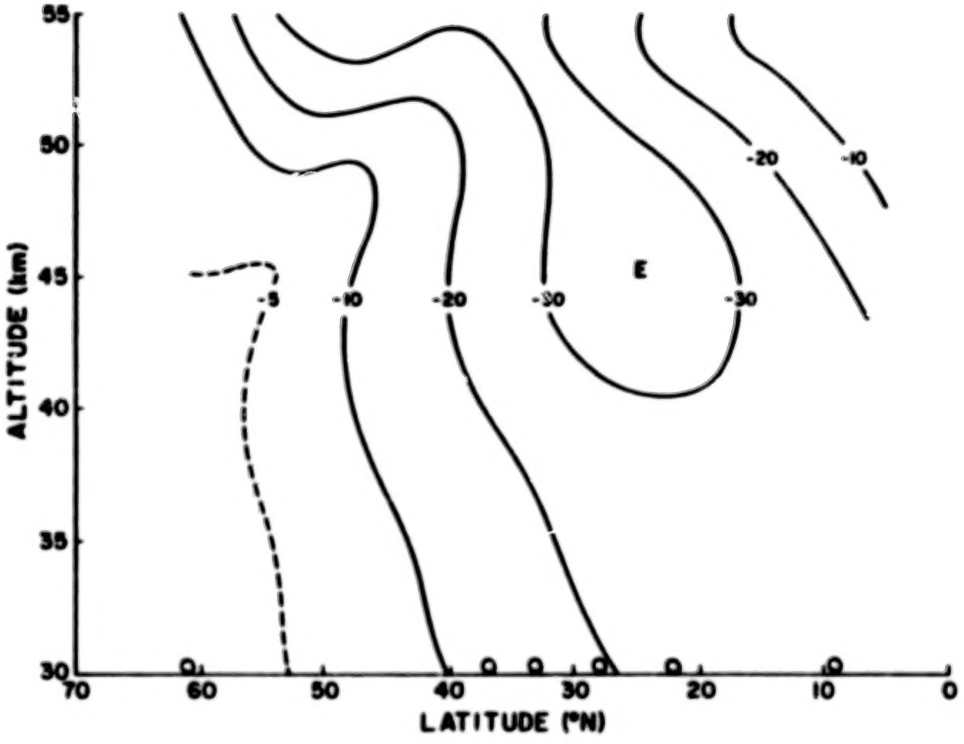

Fig. 3. Latitude-height section of the mean zonal wind (m sec^{-1}), Summer 1969-1974.

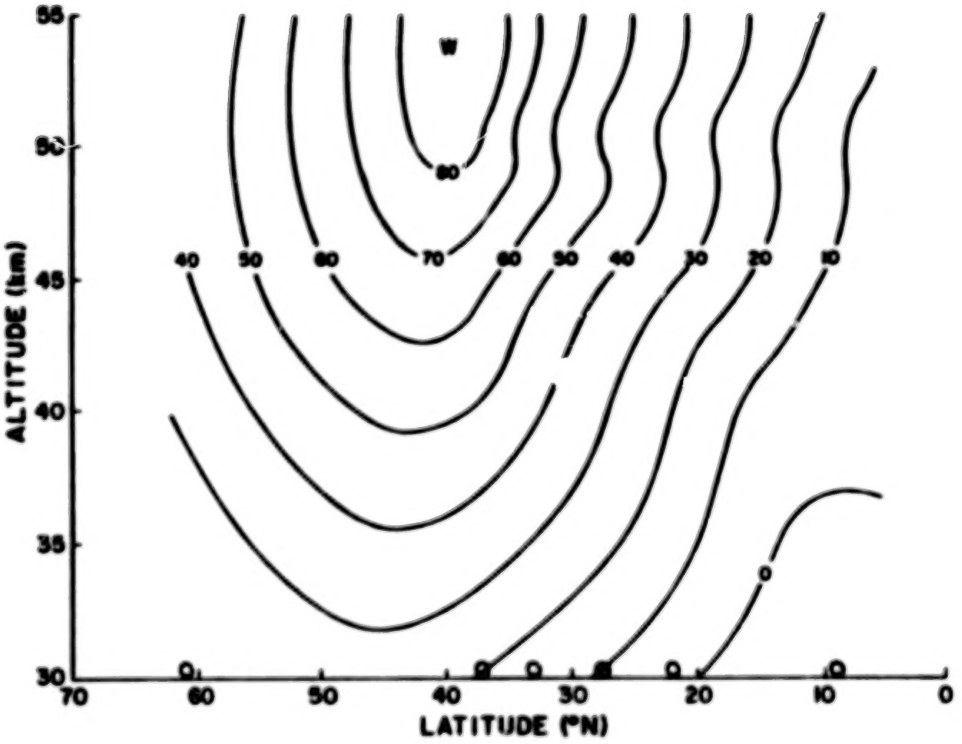

Fig. 4. Latitude-height section of the mean zonal wind (m sec^{-1}), Fall 1969-1974.

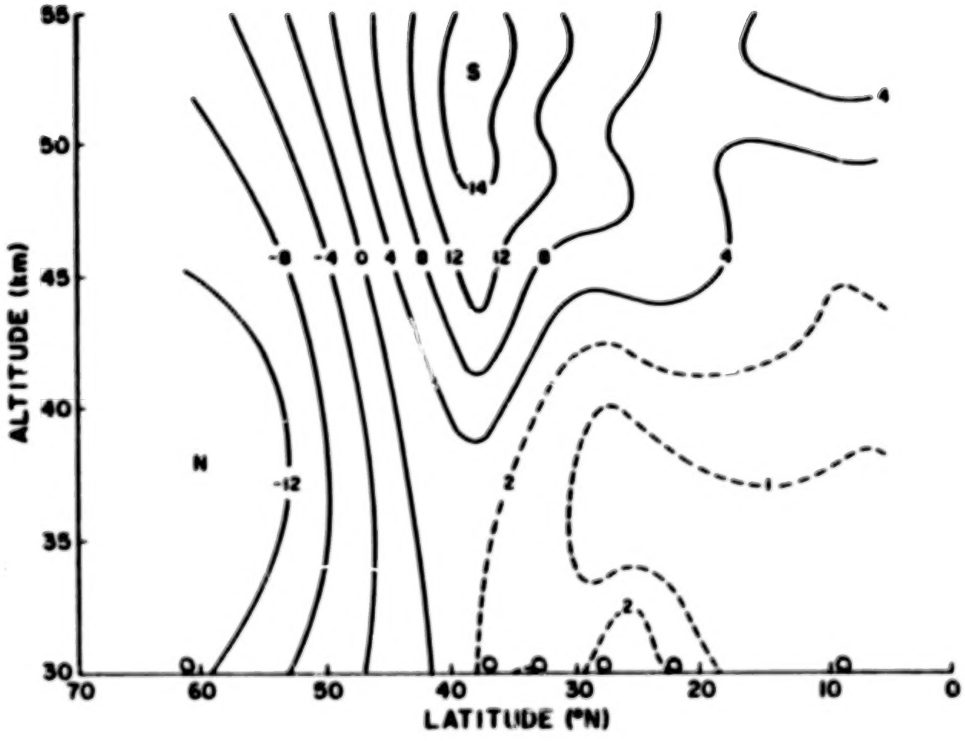

Fig. 5. Latitude-height section of the mean meridional wind (m sec^{-1}). Winter 1969-1974.

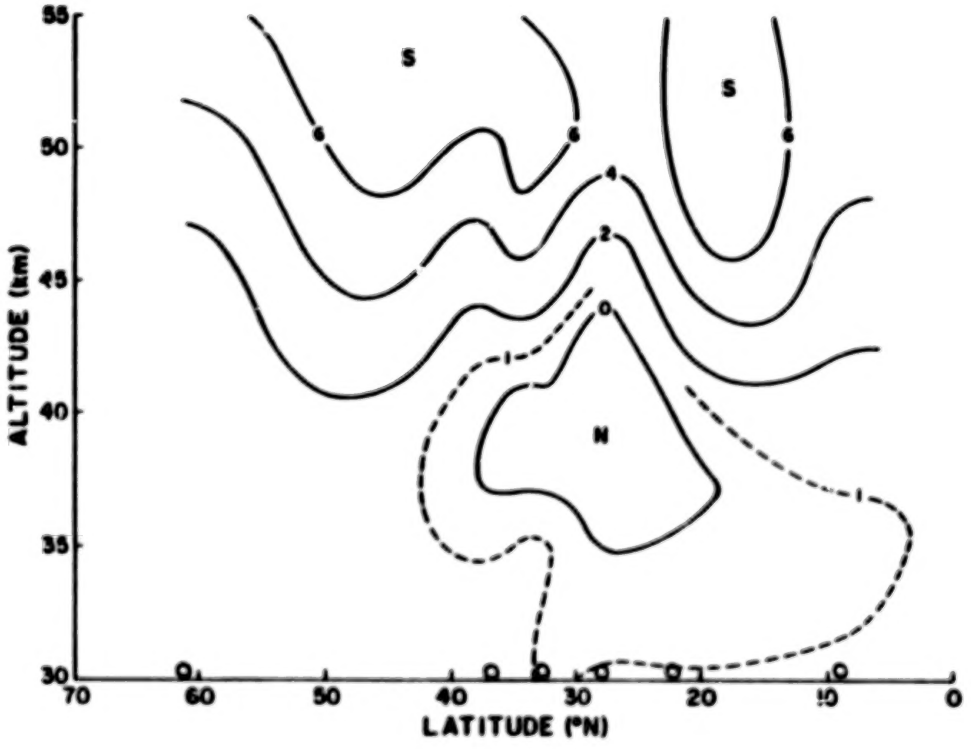

Fig. 6. Latitude-height section of the mean meridional wind (m sec^{-1}), Spring 1969-1974.

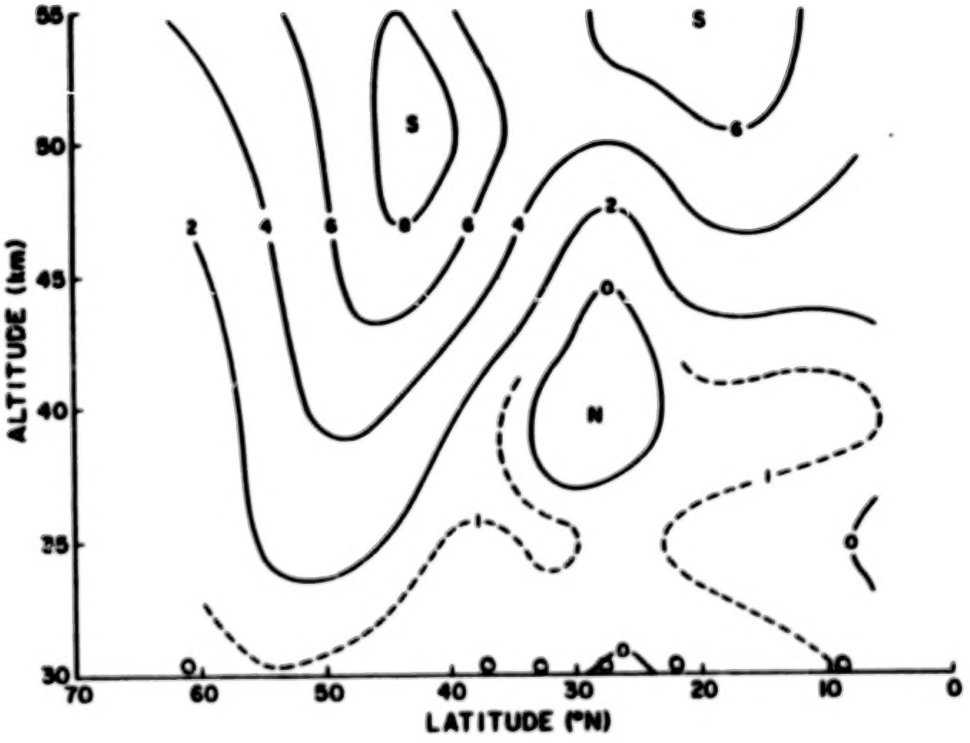

Fig. 7. Latitude-height section of the mean meridonal wind (m sec^{-1}). Summer 1969-1974.

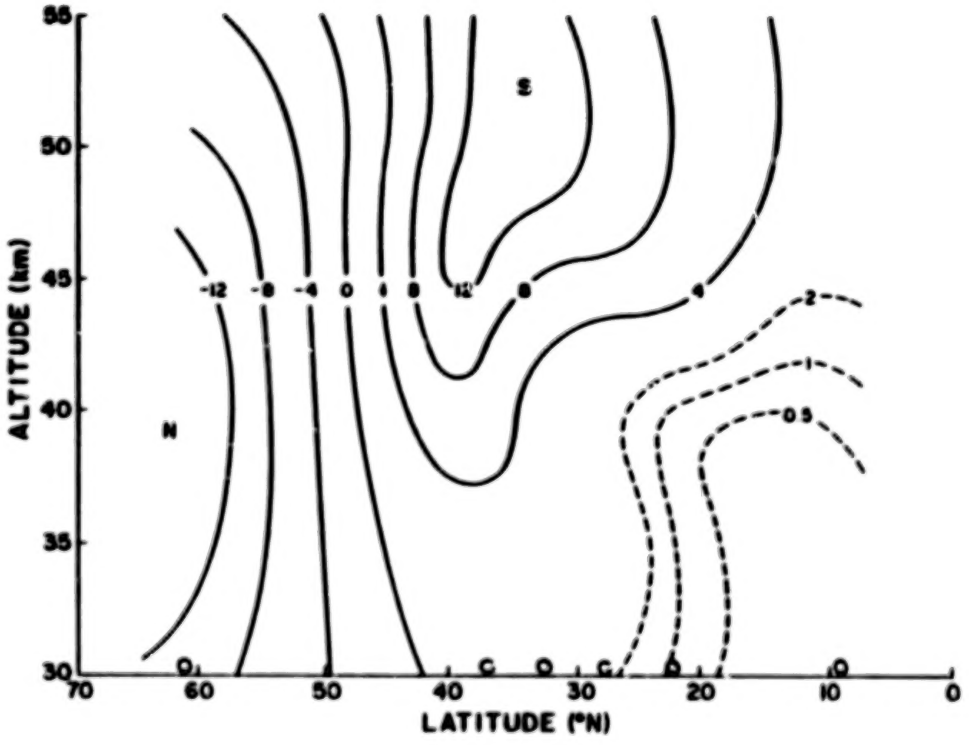

Fig. 8. Latitude-height section of the mean meridional wind (m sec^{-1}), Fall 1969-1974.

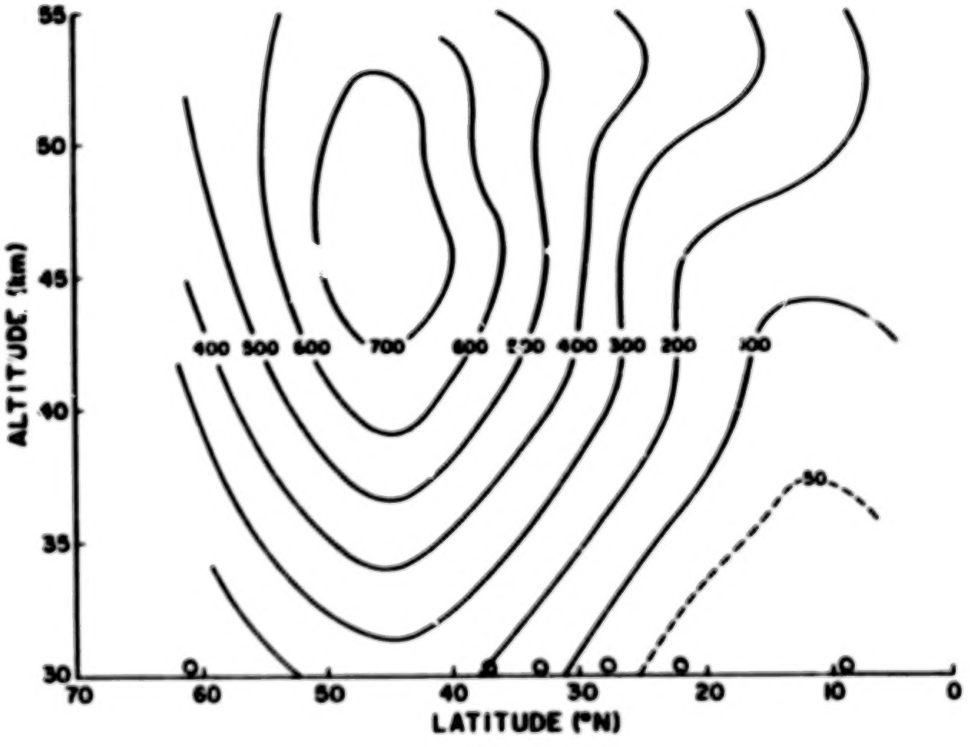

Fig. 9. Latitude-height section of the variance of the zonal wind (m^2 sec^{-2}), Winter 1969-1974.

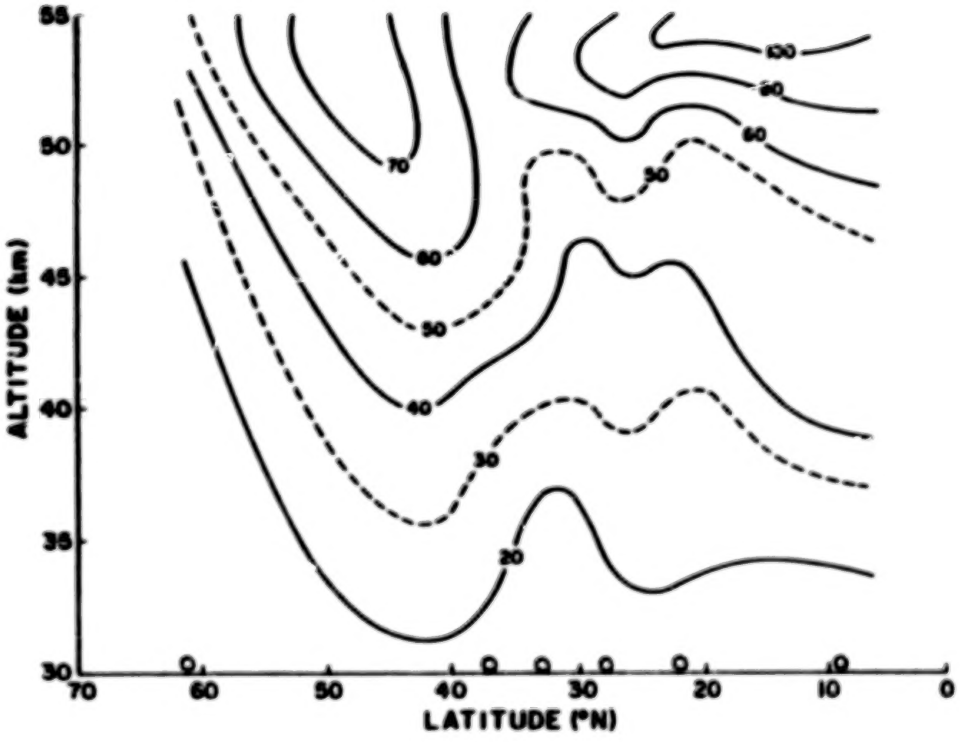

Fig. 10. Latitude-height section of the variance of the zonal wind (m^2 sec^{-2}), Spring 1969-1974.

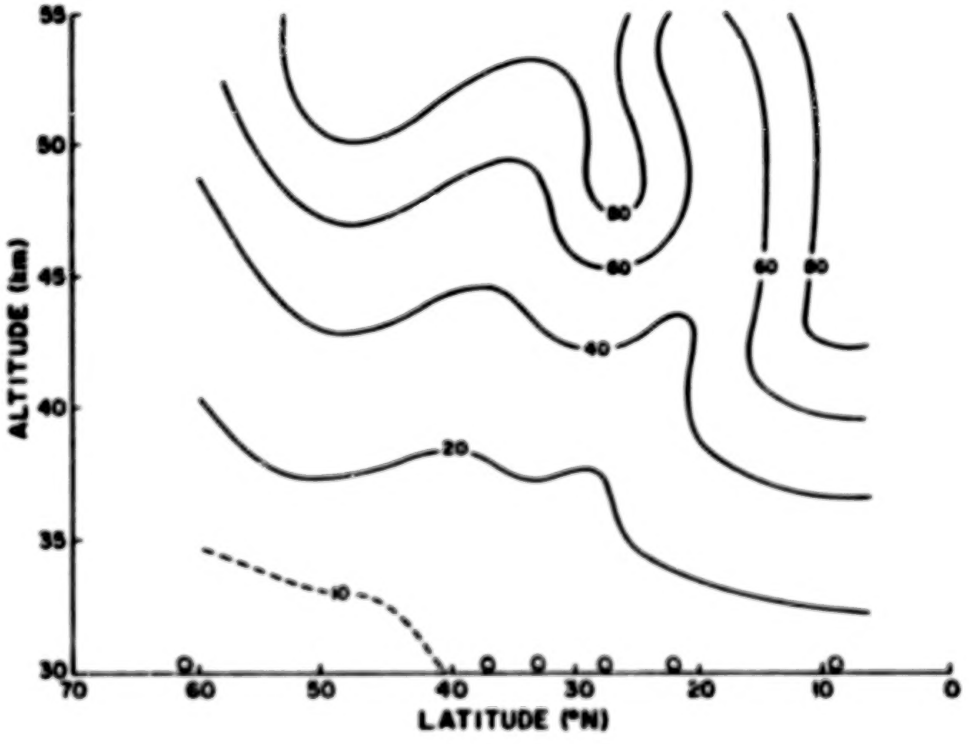

Fig. 11. Latitude-height section of the variance of the zonal wind (m^2 sec^{-2}), Summer 1969-1974.

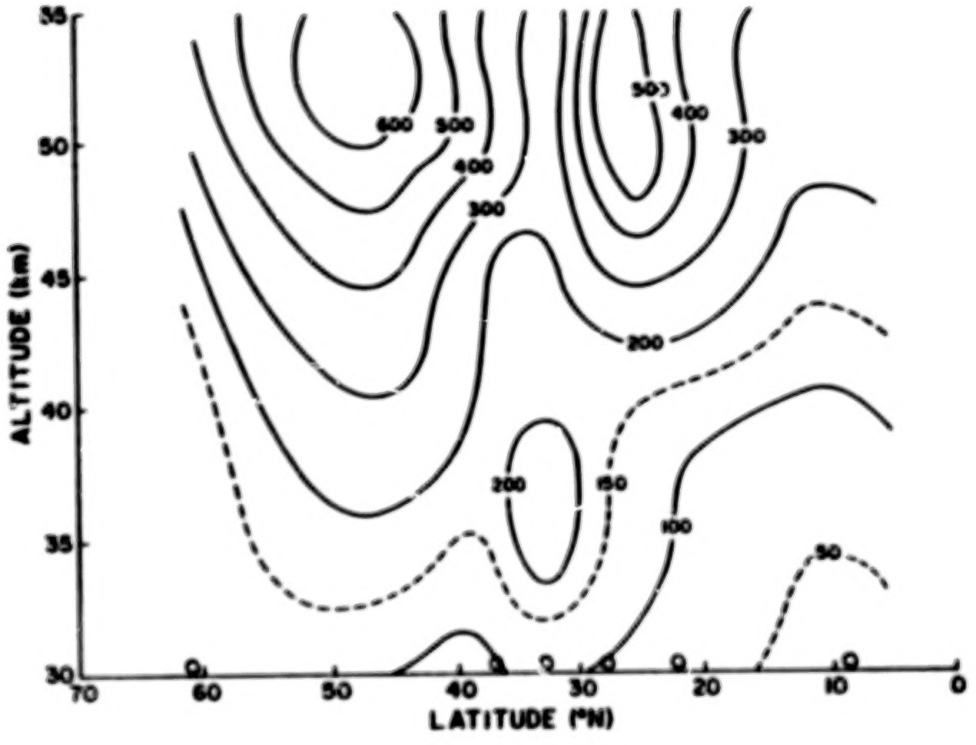

Fig. 12. Latitude-height section of the variance of the zonal wind (m^2 sec^{-2}), Fall 1969-1974.

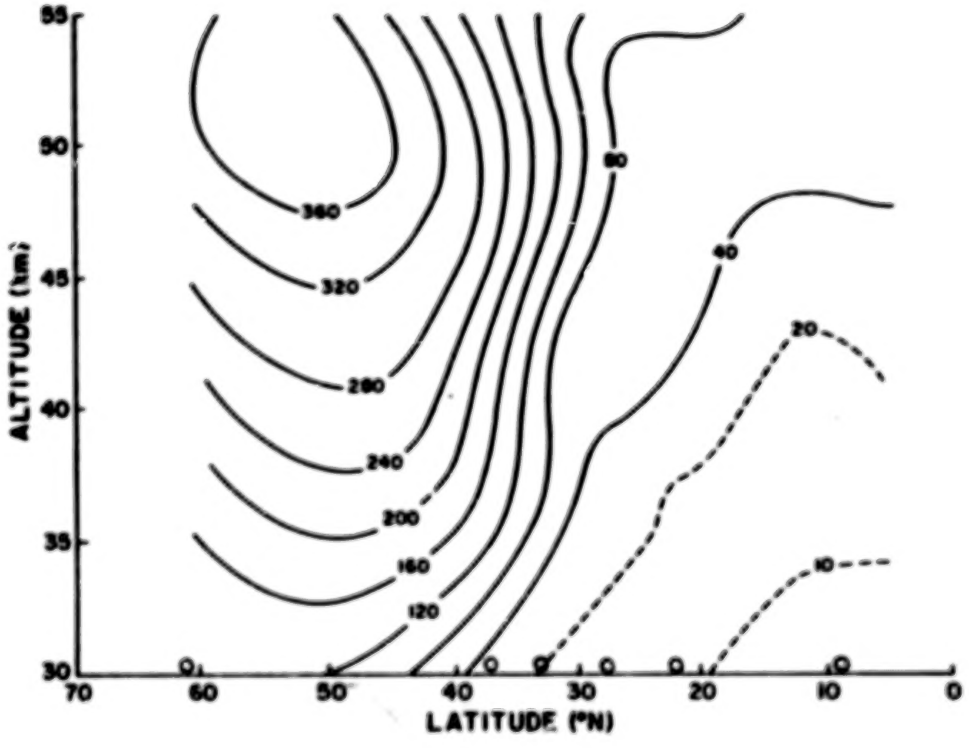

Fig. 13. Latitude-height section of the variance of the meridional wind (m^2 sec^{-2}). Winter 1969-1974.

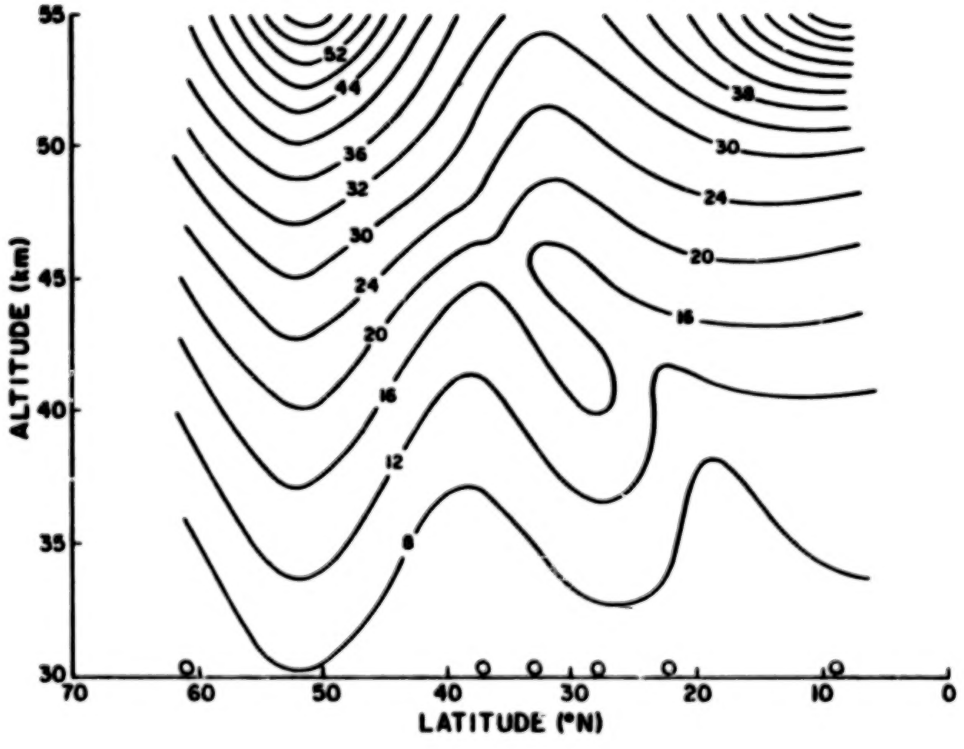

Fig. 14. Latitude-height section of the variance of the meridional wind (m^2 sec^{-2}), Spring 1969-1974.

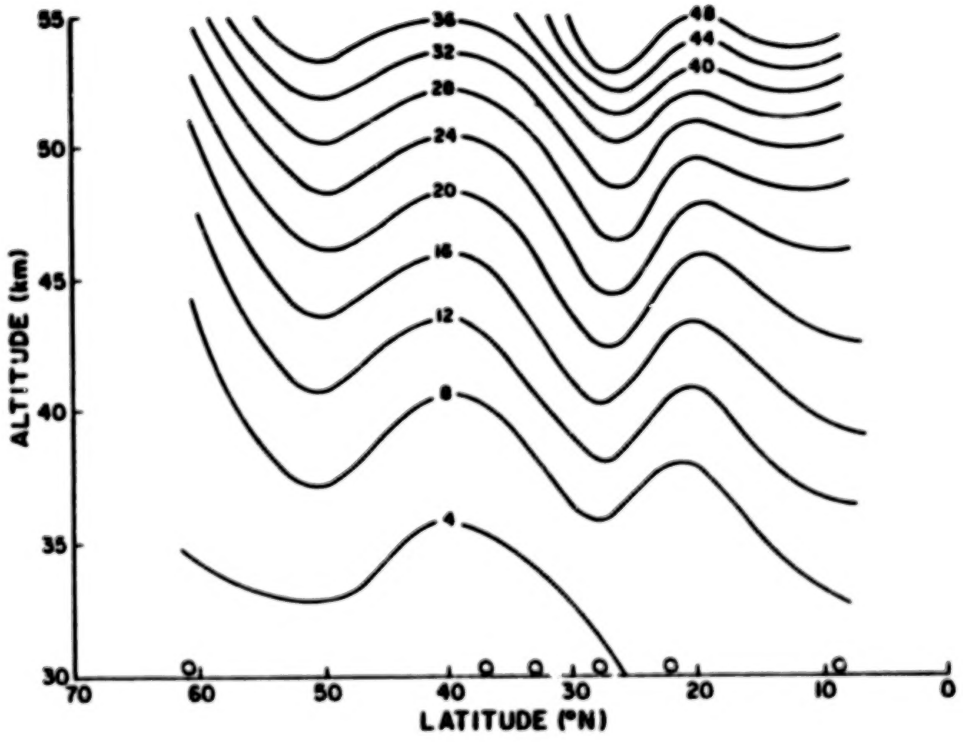

Fig. 15. Latitude-height section of the variance of the meridional wind (m^2 sec^{-2}), Summer 1969-1974.

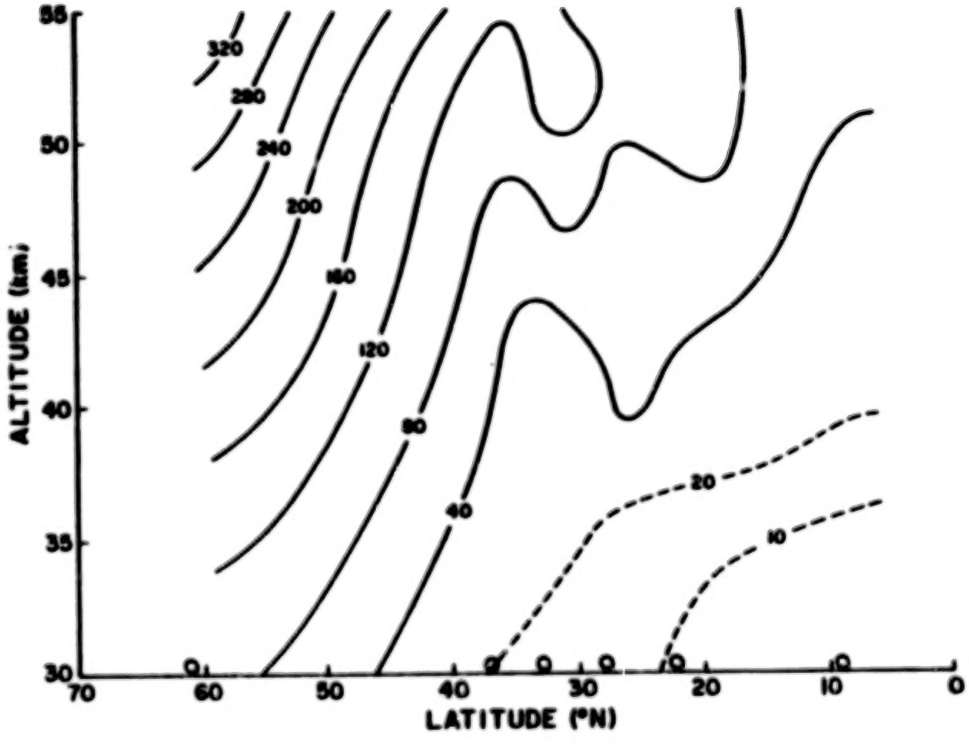

Fig. 16. Latitude-height section of the variance of the meridional wind (m^2 sec^{-2}), Fall 1969-1974.

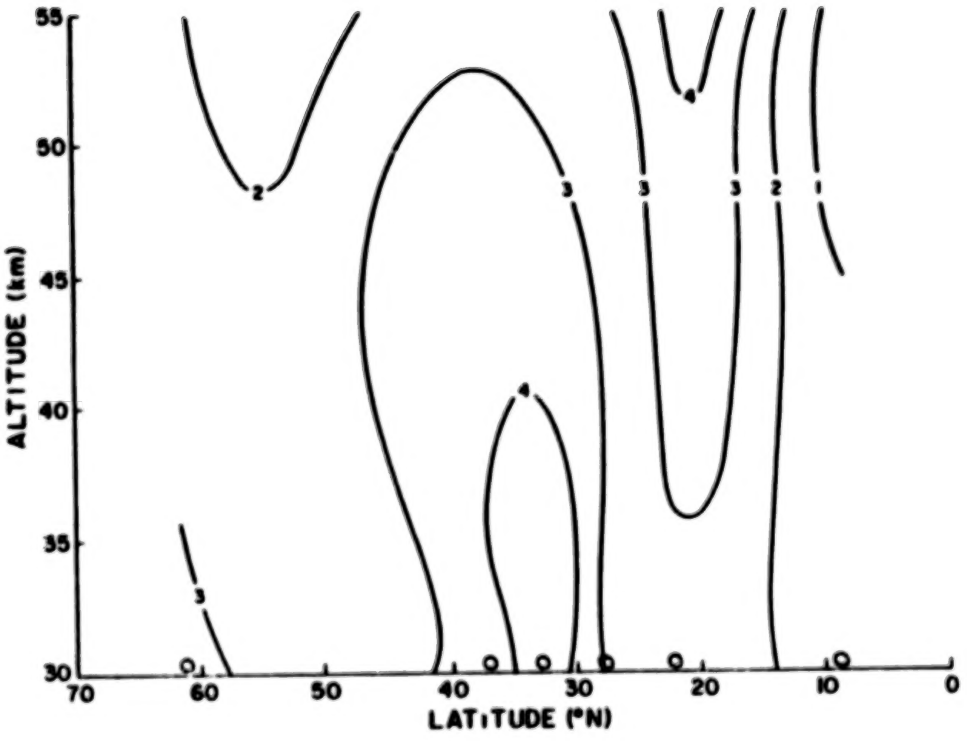

Fig. 17. Latitude-height section of the Eulerian integral time scale of the zonal component of turbulent velocity (day), Winter 1969-1974.

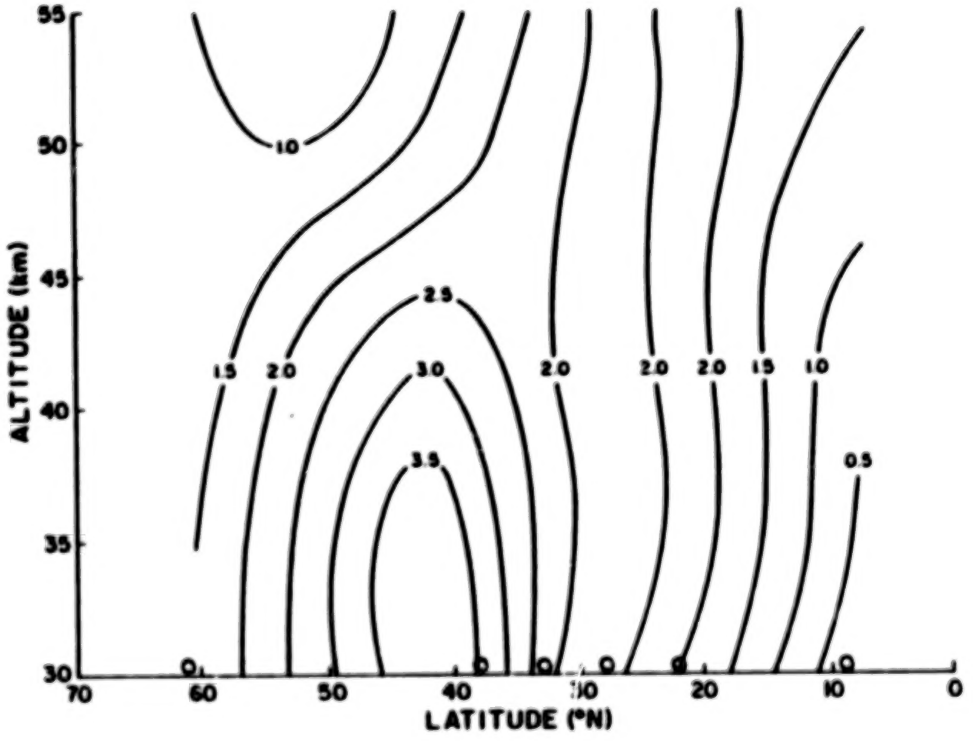

Fig. 18. Latitude-height section of the Eulerian integral time scale of the zonal component of turbulent velocity (day), Spring 1969-1974.

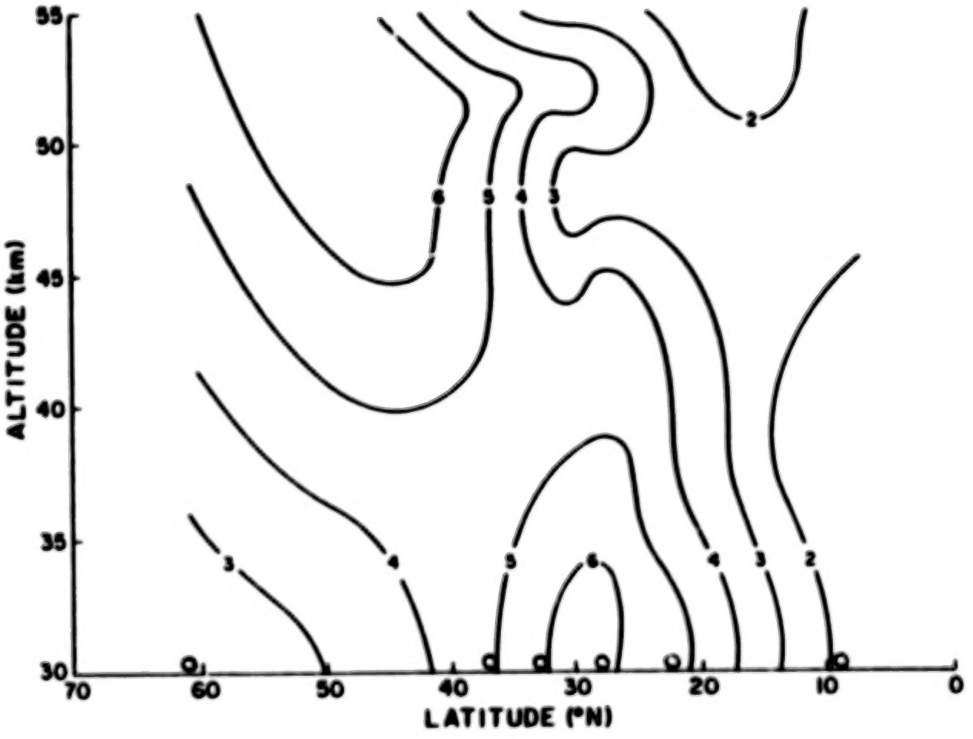

Fig. 19. Latitude-height section of the Eulerian integral time scale of the zonal component of turbulent velocity (day), Summer 1969-1974.

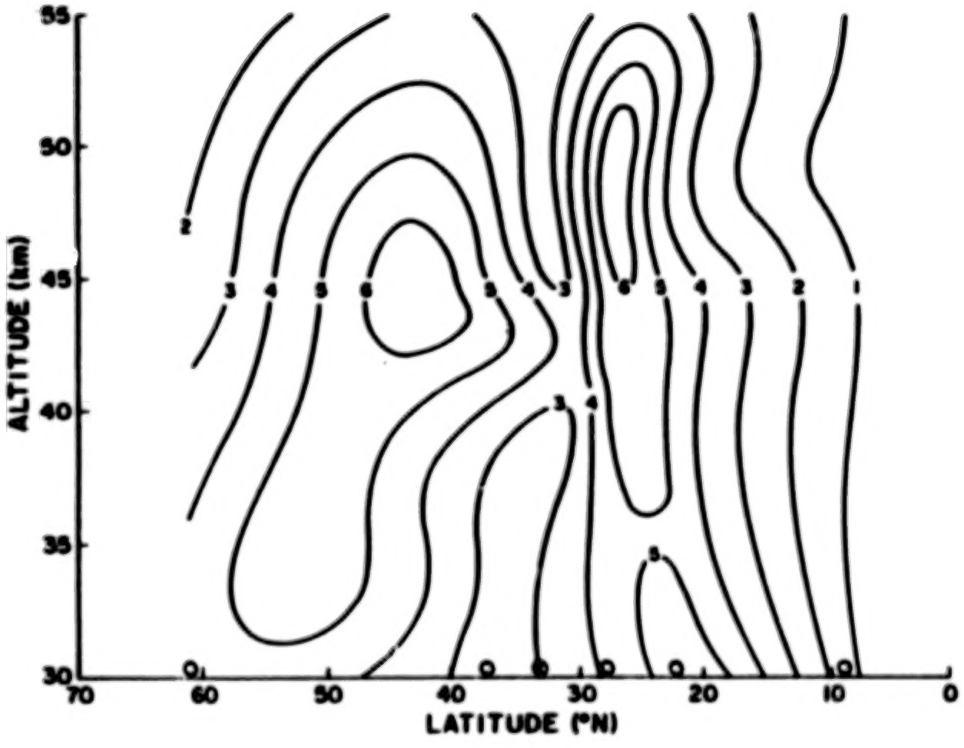

Fig. 20. Latitude-height section of the Eulerian integral time scale of the zonal component of turbulent velocity (day), Fall 1969-1974.

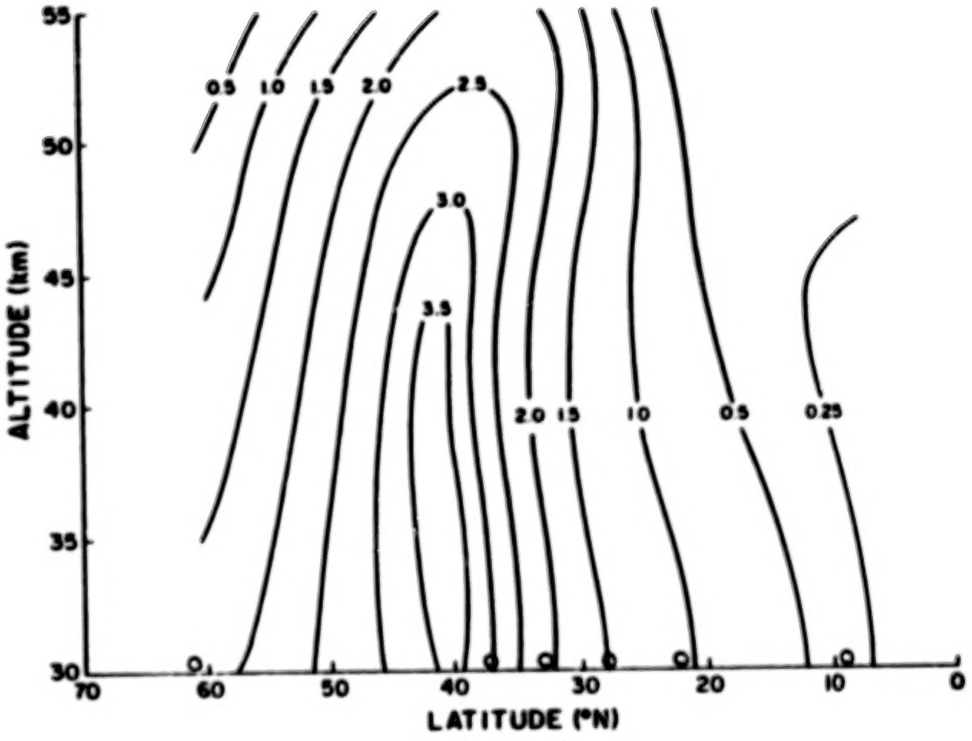

Fig. 21. Latitude-height section of the Eulerian integral time scale of the meridional component of turbulent velocity (day), Winter 1969-1974.

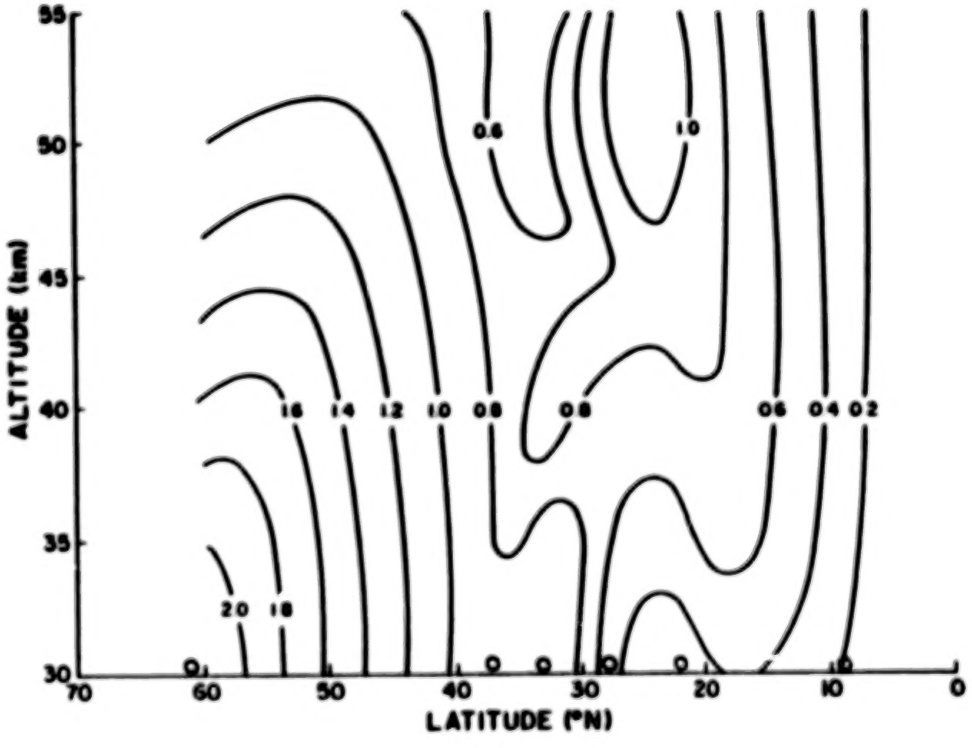

Fig. 22. Latitude-height section of the Eulerian integral time scale of the meridional component of turbulent velocity (day), Spring 1969-1974.

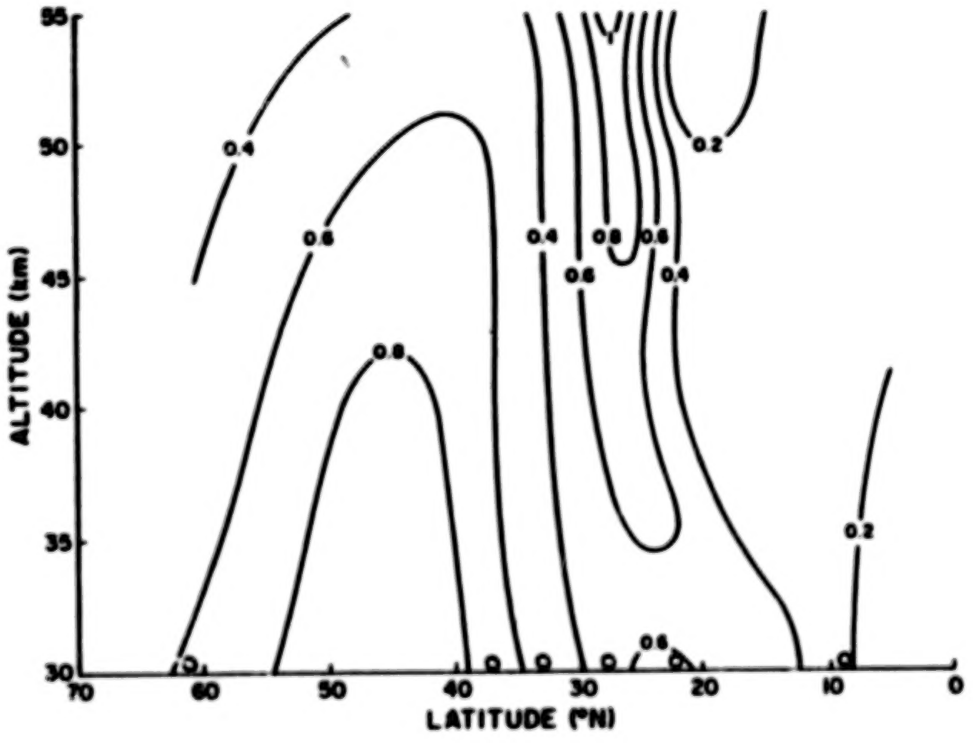

Fig. 23. Latitude-height section of the Eulerian integral time scale of the meridional component of turbulent velocity (day), Summer 1969-1974.

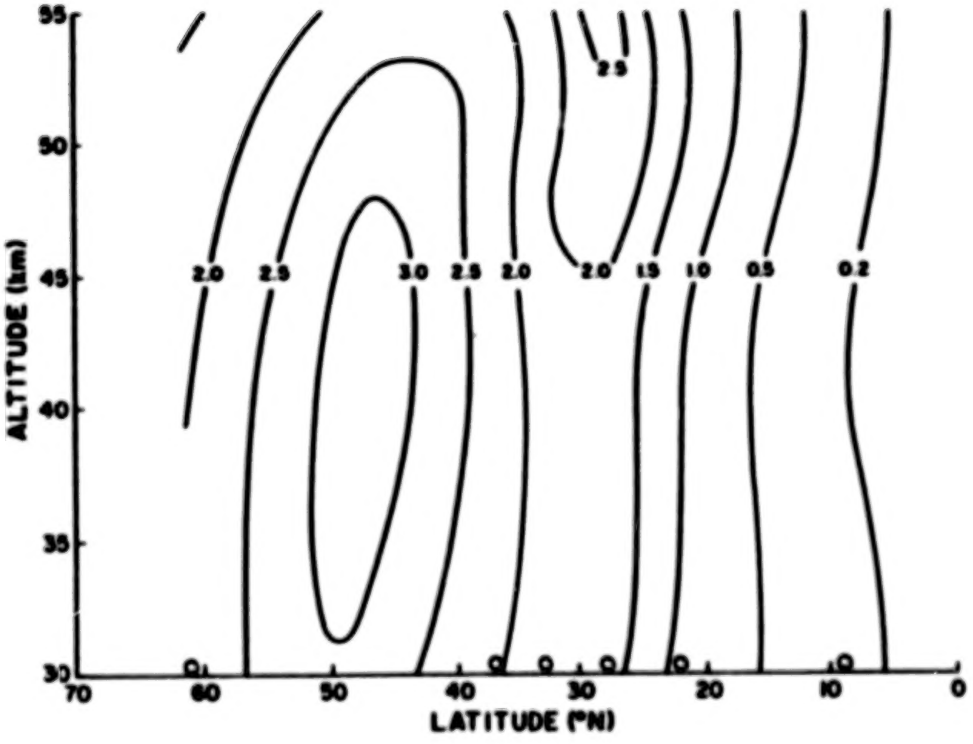

Fig. 24. Latitude-height section of the Eulerian integral time scale of the meridional component of turbulent velocity (day), Fall 1969-1974.

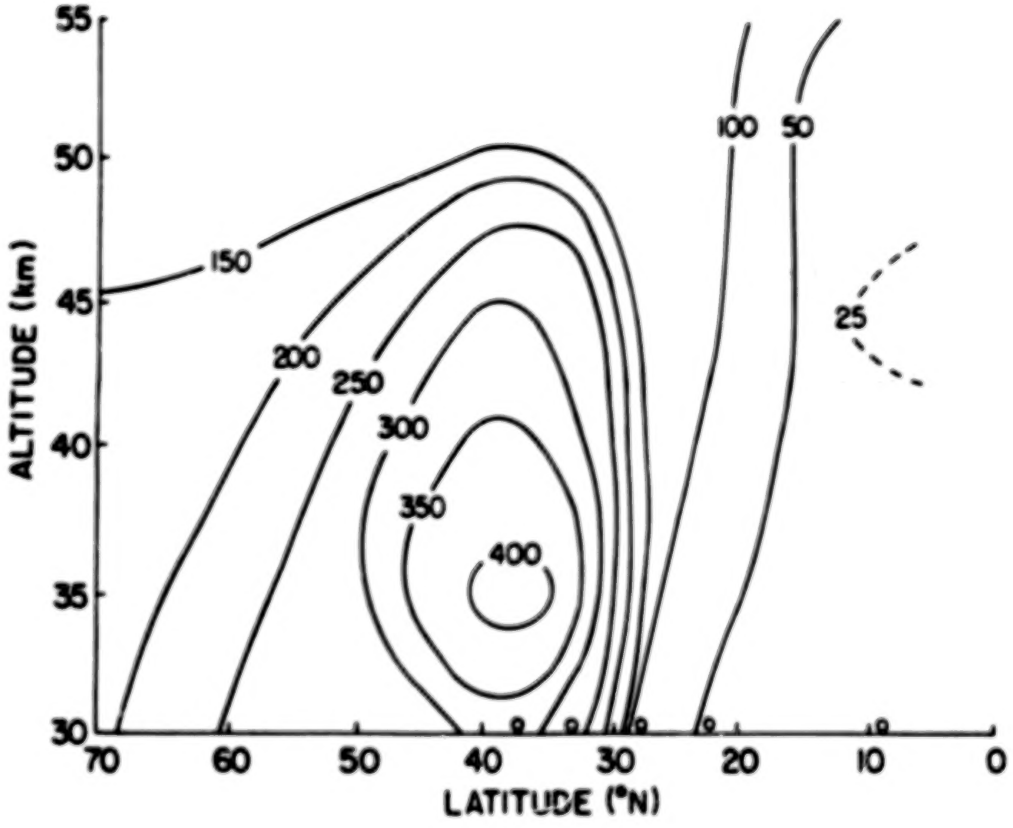

Fig. 25. Latitude-height section of the zonal component of eddy diffusivity (10^9 cm^2 sec^{-1}), Winter 1969-1974.

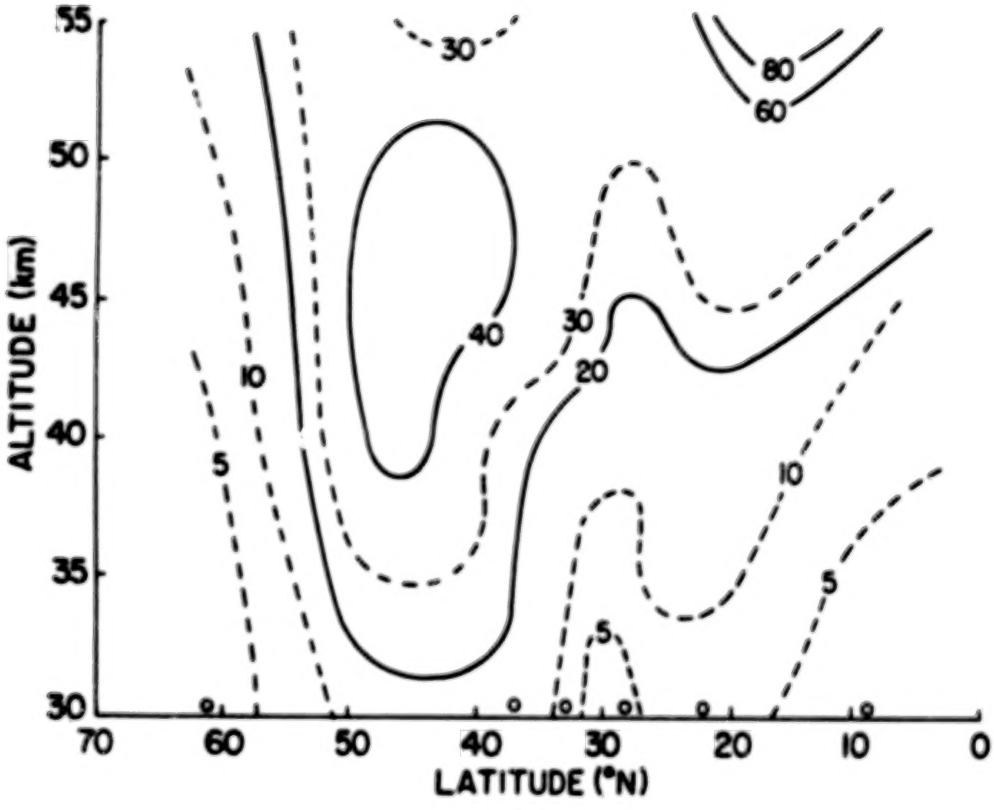

Fig. 26. Latitude-height section of the zonal component of eddy diffusivity (10^9 cm^2 sec^{-1}), Spring 1969-1974.

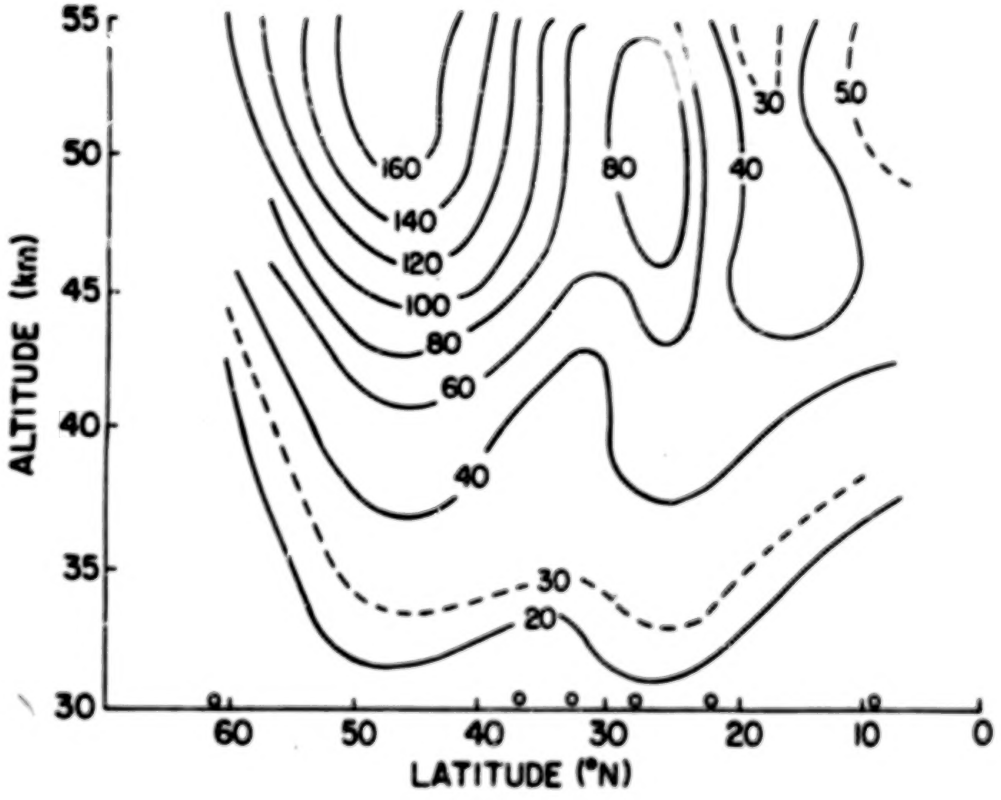

Fig. 27. Latitude-height section of the zonal component of eddy diffusivity (10^9 cm^2 sec^{-1}), Summer 1969-1974.

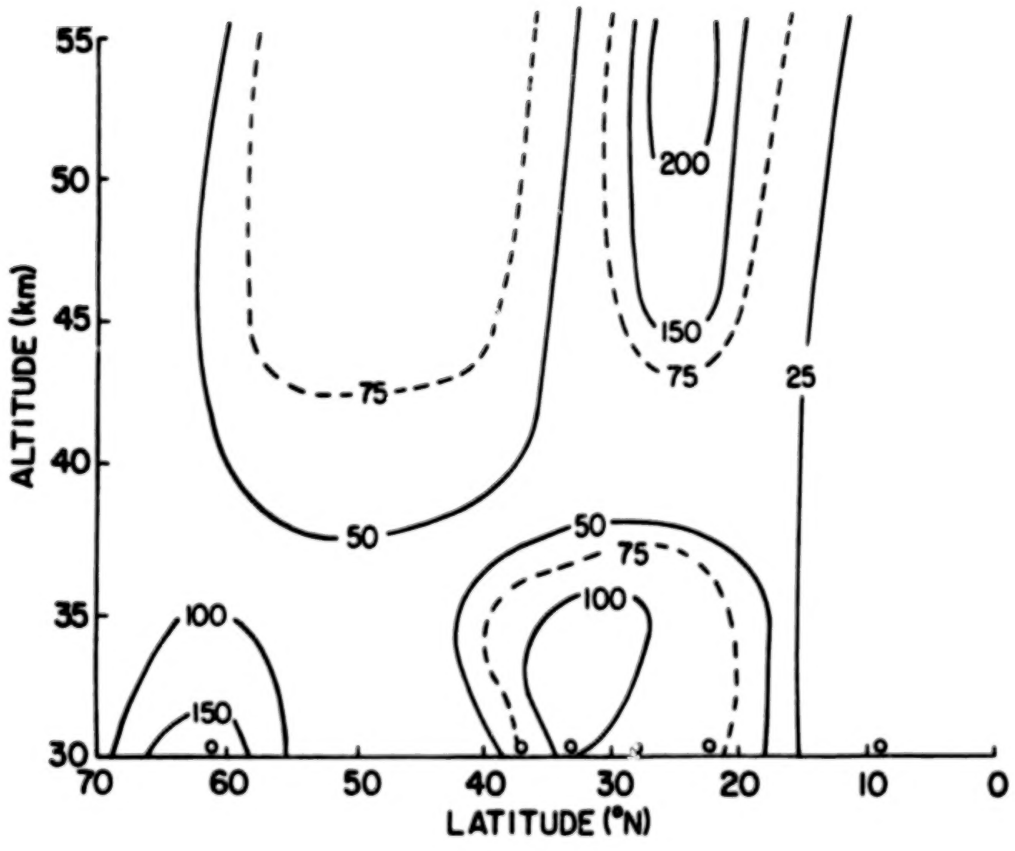

Fig. 28. Latitude-height section of the zonal component of eddy diffusivity (10^9 cm^2 sec^{-1}), Fall 1969-1974.

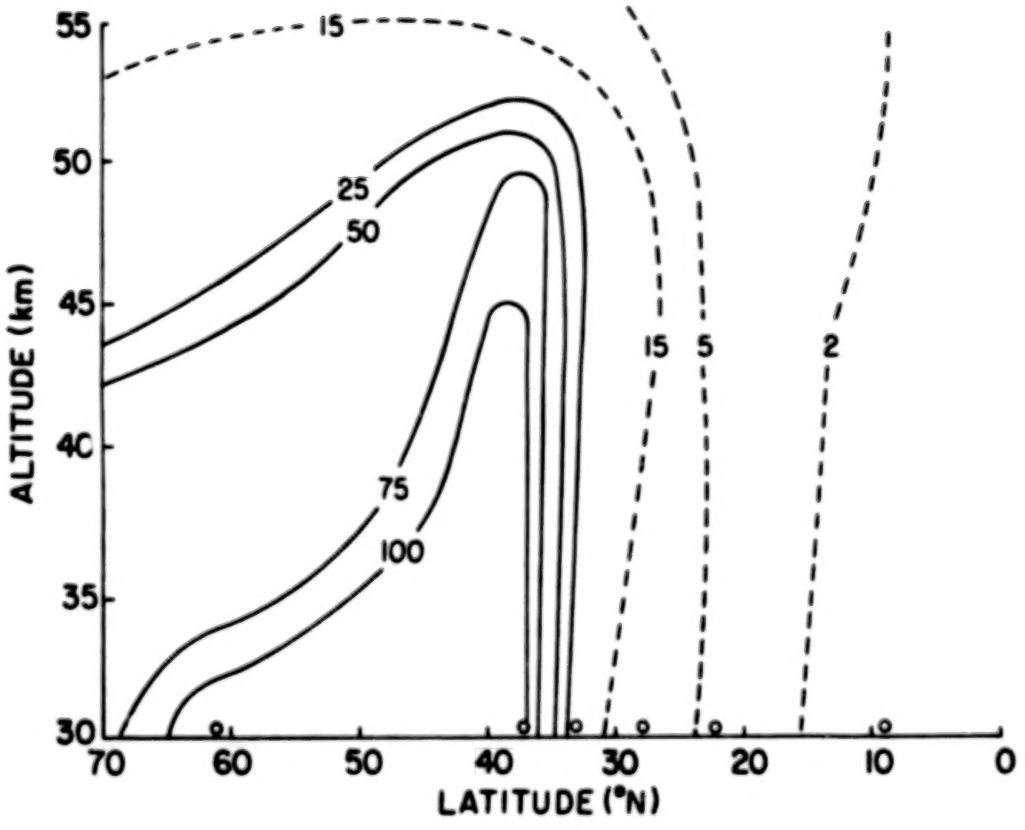

Fig. 29. Latitude-height section of the meridional component of eddy diffusivity (10^9 cm^2 sec^{-1}), Winter 1969-1974.

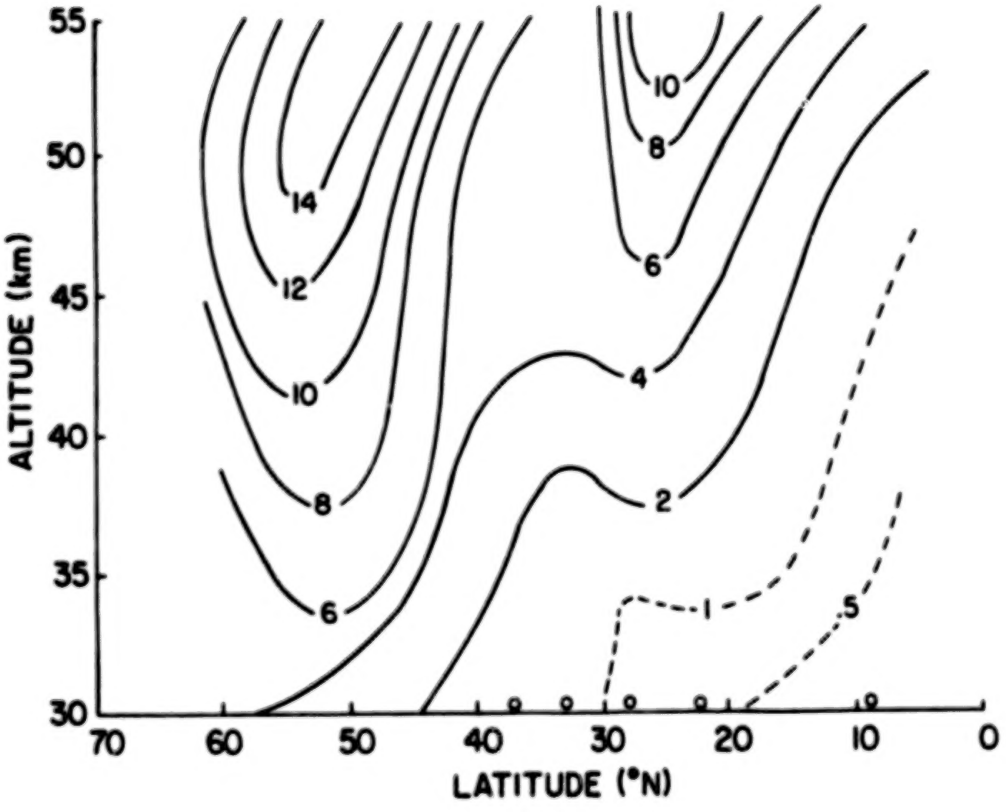

Fig. 30. Latitude-height section of the meridional component of eddy diffusivity (10^9 cm^2 sec^{-1}), Spring 1969-1974.

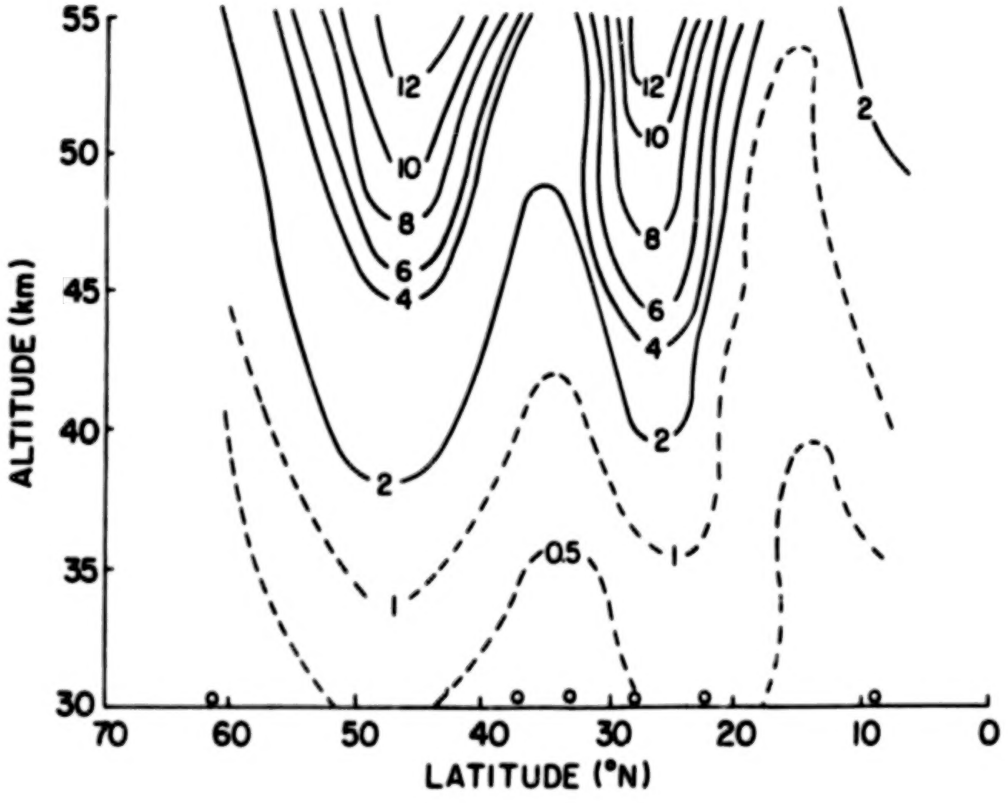

Fig. 31. Latitude-height section of the meridional component of eddy diffusivity (10^9 cm^2 sec^{-1}), Summer 1969-1974.

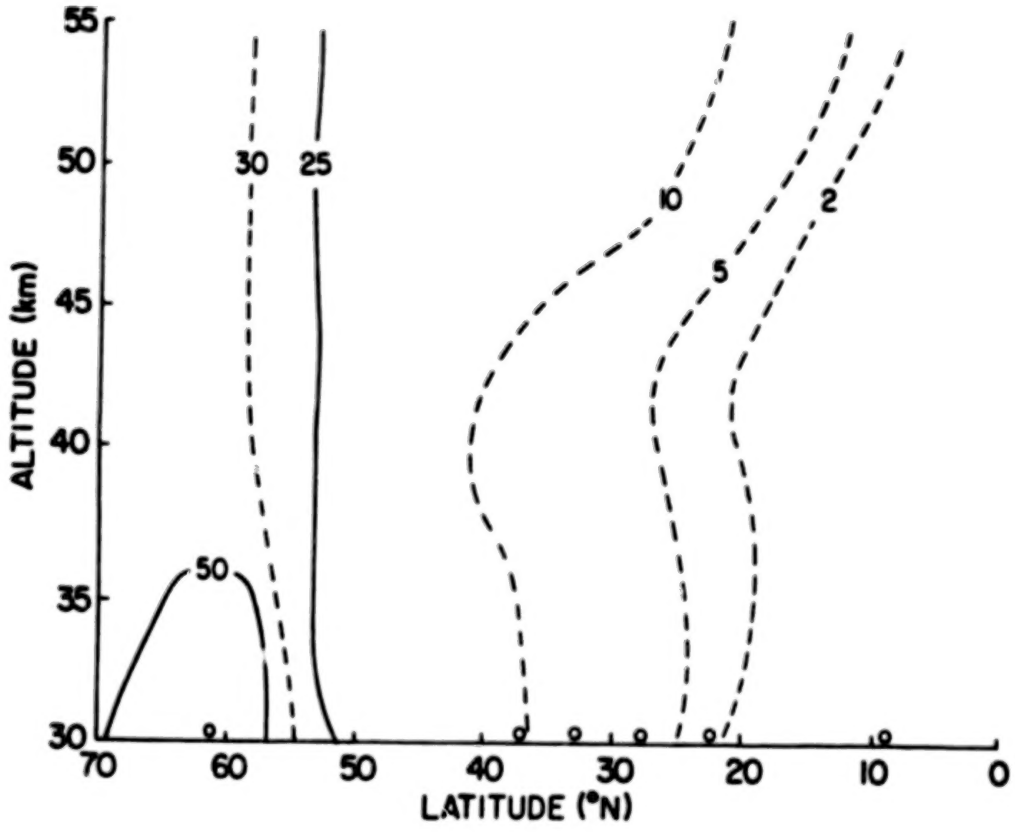

Fig. 32. Latitude-height section of the meridional component of eddy diffusivity (10^9 cm^2 sec^{-1}), Fall 1969-1974.

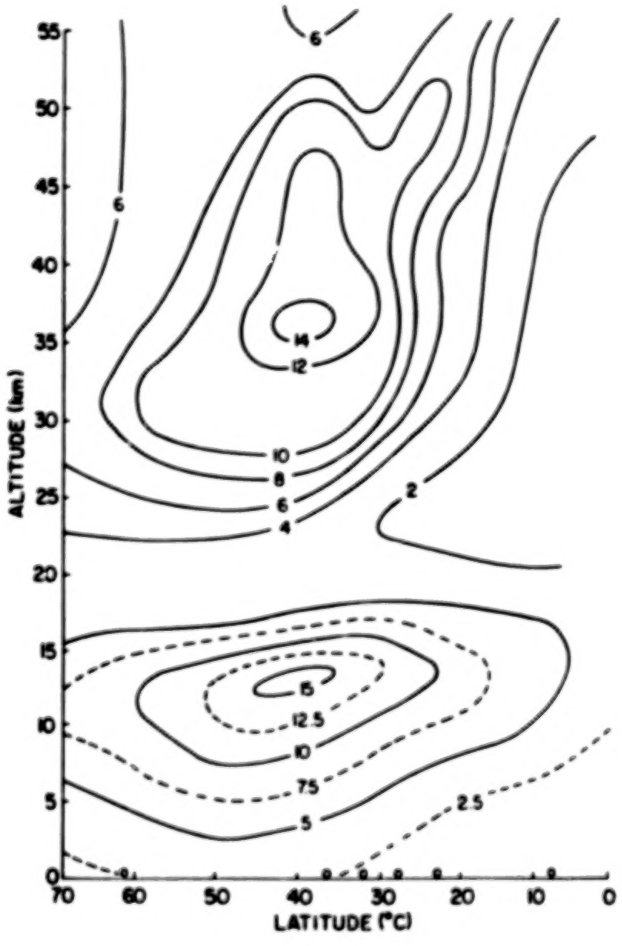

Fig. 33. Latitude-height section of the zonal component of eddy diffusivity (10^{10} cm^2 sec^{-1}), annual mean.

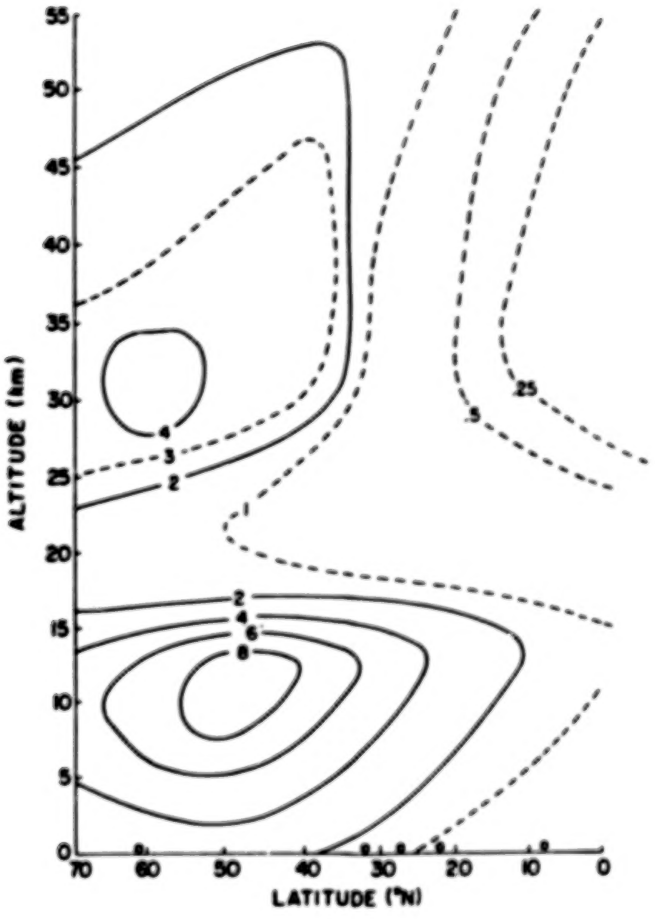

Fig. 34. Latitude-height section of the meridional component of eddy diffusivity (10^{10} cm^2 sec^{-1}), annual mean

BLANK PAGE

APPENDIX

TABLES OF THE RESULTS

Rocketsonde locations are identified by the following number:

1 = Ft. Churchill, Ft. Greely, Poker Flats
2 = Wallops Island
3 = Pt. Mugu, White Sands
4 = Cape Kennedy
5 = Barking Sands
6 = Ft. Sherman, Kwajalein

BLANK PAGE

Table 1. Mean zonal wind (m sec^{-1}), Winter 1969-1974.

Alt	Station 1	2	3	4	5	6
55	27.3	57.0	44.6	30.2	35.7	18.7
50	27.3	53.5	39.1	20.3	18.9	-1.1
45	25.4	47.4	33.5	14.5	8.8	-11.1
40	20.0	37.4	26.2	13.4	1.5	-12.5
35	15.6	28.6	18.4	17.2	6.3	-12.8
30	13.1	16.4	7.6	11.6	7.8	-5.1

Table 2. Mean zonal wind (m sec^{-1}), Spring 1969-1974.

Alt	Station 1	2	3	4	5	6
55	-15.5	-20.4	-24.2	-24.3	-20.2	-2.5
50	-9.8	-15.1	-20.0	-20.4	-20.0	-10.2
45	-7.6	-11.4	-15.2	-18.6	-22.4	-8.3
40	-7.7	-6.1	-7.9	-10.6	-17.3	-11.5
35	-7.0	-1.2	-2.2	-4.6	-14.0	-20.2
30	-6.6	-.8	-3.0	-5.5	-12.0	-17.3

Table 3. Mean zonal wind (m sec^{-1}), Summer 1969-1974.

Alt	Station 1	2	3	4	5	6
55	-12.9	-34.1	-29.8	-26.0	-14.4	-.7
50	-7.9	-28.6	-31.6	-32.8	-27.0	-10.6
45	-5.0	-26.9	-30.0	-33.8	-32.8	-21.3
40	-3.0	-21.5	-22.8	-26.1	-30.3	-27.8
35	-3.5	-15.5	-17.9	-22.4	-28.0	-26.7
30	-3.0	-13.2	-17.7	-22.8	-26.5	-22.5

Table 4. Mean zonal wind (m sec^{-1}), Fall 1969-1974.

Alt	Station 1	2	3	4	5	6
55	41.9	83.7	68.4	47.3	45.0	16.7
50	44.6	75.9	63.6	43.8	42.0	10.0
45	42.8	64.0	50.6	37.7	33.7	8.9
40	32.4	48.8	40.0	31.5	21.5	7.0
35	26.4	37.5	25.7	24.2	11.1	-2.3
30	20.4	21.4	11.3	10.4	.8	-4.0

Table 5. Mean meridonal wind (m sec^{-1}), Winter 1969-1974.

Alt	Station 1	2	3	4	5	6
55	-5.9	16.6	10.3	9.0	7.3	2.4
50	-9.2	15.7	9.8	7.4	6.4	5.3
45	-11.7	13.3	5.5	5.7	5.1	2.2
40	-15.0	6.2	.2	1.0	1.5	1.9
35	-14.3	1.7	1.4	.5	.5	.3
30	-12.5	2.5	-.1	3.1	1.2	.8

Table 6. Mean meridional wind (m sec^{-1}), Spring 1969-1974.

Alt	Station 1	2	3	4	5	6
55	5.7	6.5	5.3	4.7	7.4	4.8
50	3.8	5.3	6.5	5.3	6.2	5.2
45	1.8	3.7	3.9	1.3	5.1	2.5
40	1.9	.8	-.1	-.8	.3	1.9
35	1.5	.9	1.1	-.2	.6	.4
30	.9	1.6	1.0	1.2	1.2	1.4

Table 7. Mean meridional wind (m sec^{-1}), Summer 1969-1974.

Alt	Station 1	2	3	4	5	6
55	4.8	4.6	5.7	6.3	6.6	5.4
50	3.1	6.3	5.8	4.6	5.7	5.0
45	2.0	4.1	2.7	.4	3.8	2.9
40	1.6	1.2	.0	-.6	.3	1.0
35	1.7	.9	1.2	.7	1.5	.1
30	.8	.9	.6	-.2	.8	1.1

Table 8. Mean meridional wind (m sec^{-1}), Fall 1969-1974.

Alt	Station 1	2	3	4	5	6
55	-6.3	13.6	13.0	8.5	6.3	2.0
50	-8.7	14.9	12.9	10.0	7.5	2.7
45	-11.8	12.4	6.2	7.3	5.3	2.2
40	-14.3	5.4	1.4	2.3	.8	.7
35	-13.6	2.9	2.7	2.7	.8	.4
30	-10.3	2.7	.0	2.2	.8	.2

Table 9. Variance of the zonal wind component (m^2 sec^{-2}), Winter 1969-1974.

Alt	Station 1	2	3	4	5	6
55	547.6	479.8	447.3	339.7	346.5	197.2
50	520.7	549.0	444.1	351.6	290.9	190.5
45	414.4	536.4	502.6	272.5	215.2	152.3
40	303.5	493.3	362.0	222.3	130.7	69.4
35	215.7	371.7	233.1	139.6	62.9	49.6
30	159.0	197.5	111.5	61.0	32.9	29.3

Table 10. Variance of the zonal wind component (m^2 sec^{-2}), Spring 1969-1974.

Alt	Station 1	2	3	4	5	6
55	56.5	53.9	66.5	66.2	102.4	125.3
50	30.7	55.1	49.3	57.7	50.1	70.3
45	26.0	58.8	46.0	41.7	41.9	44.6
40	14.0	33.4	31.0	31.4	29.3	46.7
35	12.3	25.8	15.1	27.5	24.1	23.1
30	11.0	18.6	9.6	12.9	16.4	13.4

Table 11. Variance of the zonal wind component (m^2 sec^{-2}), Summer 1969-1974.

Alt	Station 1	2	3	4	5	6
55	69.7	99.0	92.4	95.1	54.7	101.9
50	42.1	72.2	65.2	92.1	55.6	87.3
45	24.7	53.5	45.2	59.4	47.2	85.0
40	19.1	24.9	28.0	32.8	41.6	62.4
35	11.0	19.7	19.1	22.6	22.4	32.4
30	7.0	13.7	14.5	13.5	11.1	15.0

Table 12. Variance of the zonal wind component (m^2 sec^{-2}), Fall 1969-1974.

Alt	Station 1	2	3	4	5	6
55	471.9	375.3	283.8	532.6	375.6	245.1
50	331.7	384.2	284.3	521.6	340.3	223.8
45	186.7	195.6	173.2	297.5	230.3	196.5
40	165.1	181.7	179.4	165.5	123.7	116.5
35	137.1	151.0	211.6	122.3	103.8	57.6
30	113.7	88.2	129.2	69.8	60.9	44.3

Table 13. Variance of the meridional wind component (m^2 sec^{-2}), Winter 1969-1974.

Alt	Station 1	2	3	4	5	6
55	344.8	231.7	136.7	86.8	92.1	57.0
50	361.2	254.0	134.1	81.5	61.2	67.2
45	305.8	250.1	118.6	61.9	42.2	30.8
40	218.0	182.5	56.8	46.9	30.1	17.5
35	160.3	122.1	30.1	30.2	15.5	12.4
30	127.2	69.1	11.5	19.6	11.1	6.0

Table 14. Variance of the meridional wind component (m^2 sec^{-2}), Spring 1969-1974.

Alt	Station 1	2	3	4	5	6
55	41.9	39.3	29.2	34.6	39.2	63.0
50	35.4	26.1	22.5	23.4	23.5	28.5
45	22.6	16.9	14.4	16.7	18.1	18.2
40	14.9	13.5	11.1	16.0	11.6	11.7
35	8.1	6.2	9.0	9.0	7.8	10.5
30	4.3	5.7	5.4	7.0	4.7	6.8

Table 15. Variance of the meridional wind component (m^2 sec^{-2}), Summer 1969-1974.

Alt	Station 1	2	3	4	5	6
55	26.4	36.6	42.3	63.6	47.5	52.1
50	14.2	23.0	27.5	33.2	28.5	31.9
45	10.7	16.1	18.1	27.7	18.5	21.2
40	4.7	7.5	11.0	15.2	10.7	16.5
35	4.4	4.6	4.7	6.9	6.6	9.2
30	2.6	3.0	2.8	4.1	4.3	6.9

Table 16. Variance of the meridional wind component (m^2 sec^{-2}), Fall 1969-1974.

Alt	Station 1	2	3	4	5	6
55	337.5	129.3	128.5	88.8	92.4	55.7
50	280.6	107.8	123.1	81.2	85.2	39.7
45	233.0	67.3	62.9	60.8	54.9	36.1
40	176.7	43.8	39.0	42.1	28.0	21.7
35	146.4	30.7	29.9	19.1	17.6	9.7
30	92.7	18.9	14.0	12.5	8.2	6.7

Table 17. Eulerian integral time scale of the zonal component of turbulent velocity (day), Winter 1969-1974.

Alt	Station 1	2	3	4	5	6
55	1.97	-	2.51	2.74	4.04	.83
50	2.22	3.54	2.98	2.77	3.78	.94
45	2.47	3.55	3.45	2.80	3.52	1.05
40	2.73	3.56	3.91	2.82	3.26	1.16
35	2.98	3.57	4.38	2.85	3.00	1.27
30	3.23	3.58	4.84	2.88	2.74	1.38

Table 18. Eulerian integral time scale of the zonal component of turbulent velocity (day), Spring 1969-1974.

Alt	Station 1	2	3	4	5	6
55	1.01	1.58	2.26	1.63	2.79	1.69
50	1.17	1.96	2.23	1.67	2.62	1.38
45	1.34	2.33	2.20	1.70	2.45	1.07
40	1.50	2.70	2.18	1.73	2.28	.76
35	1.66	3.08	2.15	1.77	2.11	.46
30	1.83	3.45	2.12	1.80	1.94	.15

Table 19. Eulerian integral time scale of the zonal component of turbulent velocity (day), Summer 1969-1974.

Alt	Station 1	2	3	4	5	6
55	6.10	-	2.54	2.84	1.65	2.31
50	5.42	5.37	3.24	3.51	3.26	2.17
45	4.75	5.10	3.95	4.17	3.07	2.04
40	4.07	4.84	4.65	4.84	3.77	1.90
35	3.40	4.57	5.36	5.50	4.48	1.76
30	2.72	-	6.06	6.16	5.19	1.62

Table 20. Eulerian integral time scale of the zonal component of turbulent velocity (day), Fall 1969-1974.

Alt	Station 1	2	3	4	5	6
55	1.41	-	2.49	-	2.75	1.01
50	2.11	-	2.68	6.64	3.25	1.02
45	2.80	5.04	2.87	6.01	3.76	1.02
40	3.50	4.03	3.06	5.39	4.27	1.03
35	4.19	3.02	3.25	4.76	4.78	1.03
30	4.88	2.01	3.44	4.13	5.28	1.04

Table 21. Eulerian integral time scale of the meridional component of turbulent velocity (day), Winter 1969-1974.

Alt	Station 1	2	3	4	5	6
55	.39	-	1.91	1.01	.32	.32
50	.68	2.69	1.81	1.15	.47	.30
45	.97	2.81	1.70	1.28	.62	.28
40	1.25	2.92	1.60	1.42	.77	.26
35	1.54	3.04	1.50	1.56	.92	.24
30	1.83	3.16	1.40	1.69	1.07	.22

Table 22. Eulerian integral time scale of the meridional component of turbulent velocity (day), Spring 1969-1974.

Alt	Station 1	2	3	4	5	6
55	.72	.61	.50	1.15	.98	.24
50	1.02	.68	.61	1.00	.89	.24
45	1.33	.75	.71	.86	.81	.24
40	1.63	.81	.82	.71	.72	.24
35	1.94	.88	.92	.56	.64	.24
30	2.24	.95	1.03	.41	.55	.23

Table 23. Eulerian integral time scale of the meridional component of turbulent velocity (day), Summer 1969-1974.

Alt	Station 1	2	3	4	5	6
55	.37	.59	.42	1.11	.12	.36
50	.43	.61	.43	.99	.23	.34
45	.49	.63	.44	.88	.33	.31
40	.56	.65	.45	.76	.44	.28
35	.62	.67	.46	.65	.54	.26
30	.68	.70	.47	.53	.65	.23

Table 24. Eulerian integral time scale of the meridional component of turbulent velocity (day), Fall 1969-1974.

Alt	Station 1	2	3	4	5	6
55	1.54	-	1.88	2.40	1.31	.28
50	1.73	2.38	1.88	2.25	1.21	.27
45	1.92	2.31	1.89	2.09	1.10	.26
40	2.11	2.25	1.89	1.94	.99	.25
35	2.31	2.18	1.89	1.78	.88	.24
30	2.50	2.12	1.89	1.63	.77	.23

Table 25. Zonal Component of Eddy Diffusivity (10^9 $Cm^2 \cdot sec^{-1}$), Annual Average, 1969 - 1974

ALT	Station 1	2	3	4	5	6
55	74.3	59.0	69.0	63.5	81.2	40.8
50	61.0	98.5	70.6	115.3	66.5	29.3
45	61.4	123.6	98.5	86.2	80.8	25.9
40	62.7	123.8	101.2	66.5	49.3	17.7
35	86.5	149.3	130.5	72.5	50.0	13
30	105.3	108.5	105.5	50.0	40.8	10.3

Table 26. Meridional Component of Eddy Diffusivity ($10^9 Cm^2 \cdot sec^{-1}$), Annual Average, 1969 - 1974

ALT	Station 1	2	3	4	5	6
55	15.4	13.3	13.3	11.1	6.0	3.2
50	17.8	24.4	12.1	9.7	4.5	1.3
45	22.6	32.6	11.6	8.4	3.7	1.3
40	24.0	31.8	7.3	7.0	2.7	.9
35	38.3	36.2	7.3	6.6	2.6	.7
30	45.8	30.0	4.4	66.2	2.3	.5

Table 27. Zonal Component of Eddy Diffusivity, (10^9 $Cm^2 \cdot sec^{-1}$), Winter 1969 - 1974

ALT	Station 1	2	3	4	5	6
55	112.0		116.0	97.0	145.2	16.9
50	119.8	201.3	137.2	101.0	114.0	18.5
45	163.7	304.0	276.9	121.8	121.0	25.5
40	17?.9	377.5	304.7	135.1	91.6	17.2
35	225.3	465.0	358.1	139.6	66.1	22.0
30	249.9	343.5	262.8	85.5	43.7	19.6

Table 28. Zonal Component of eddy diffusivity (10^9 cm^2 sec^{-1}), Spring 1969-1974

ALT	Station 1	2	3	4	5	6
55	16.5	24.6	43.3	31.2	82.2	61.2
50	10.2	31.1	31.7	27.7	37.8	28.1
45	9.6	39.4	29.2	20 4	29.6	13.8
40	5.7	26.0	19.4	15.7	19.2	10.3
35	5.5	22.8	9.4	14.0	14.7	3.0
30	5.4	18.5	5.9	6.7	9.2	.6

Table 29. Zonal component of eddy diffusivity (10^9 cm^2 sec^{-1}), Summer 1969 - 1974

Alt	Station 1	2	3	4	5	6
55	122.4	-	67.6	77.9	26.0	67.8
50	65.7	111.7	60.9	93.1	37.1	54.7
45	33.8	78.7	51.4	71.4	41.6	49.8
40	22.4	34.7	37.5	45.6	45.2	34.1
35	10.7	25.9	29.5	35.8	28.9	16.4
30	5.5	-	25.3	23.9	16.6	7.0

Table 30. Zonal component of eddy diffusivity (10^9 cm^2 sec^{-1}), Fall 1969 - 1974

Alt	Station 1	2	3	4	5	6
55	46.1	-	48.7	-	71.3	17.1
50	48.3	-	52.5	239.3	76.5	15.7
45	38.4	72.4	36.4	131.3	63.6	14.7
40	44.9	56.9	42.6	69.3	41.0	9.3
35	104.2	82.8	124.6	100.0	90.0	10.7
30	159.9	51.1	127.9	83.1	92.6	13.3

Table 31. Meridional component of eddy diffusivity (10^9 $cm^2 \cdot sec^{-1}$), Winter 1969 - 1974

Alt	Station 1	2	3	4	5	6
55	14.1	-	27.0	9.1	3.0	1.9
50	25.5	70.9	25.1	9.9	3.0	2.1
45	47.3	112.3	32.3	13.2	4.2	1.4
40	58.9	114.8	19.6	15.1	5.0	1.0
35	86.7	130.2	15.8	17.5	5.0	1.1
30	113.2	106.1	7.8	17.4	5.7	.7

Table 32. Meridional component of eddy diffusivity (10^9 cm^2 sec^{-1}), Spring 1969 - 1974

Alt	Station 1	2	3	4	5	6
55	8.7	6.9	4.2	11.5	11.0	4.3
50	10.4	5.1	3.9	6.8	6.0	1.9
45	8.7	3.6	3.0	4.1	4.2	1.2
40	7.0	3.2	2.6	3.3	2.4	.8
35	4.5	1.6	2.4	1.4	1.4	.7
30	2.7	1.6	1.6	.8	.7	.5

Table 33. Meridional component of eddy diffusivity (10^9 cm^2 sec^{-1}), Summer 1969 - 1974

Alt	Station 1	2	3	4	5	6
55	2.8	6.2	5.1	20.3	1.7	5.4
50	1.8	4.0	3.4	9.5	1.9	3.1
45	1.5	2.9	2.3	7.0	1.8	1.9
40	.8	1.4	1.4	3.3	1.3	1.3
35	.8	.9	.6	1.3	1.0	.7
30	.5	.6	.4	.6	.8	.5

Table 34. Component of eddy diffusivity (10^9 cm^2 sec^{-1}), Fall 1969-1974

Alt	Station 1	2	3	4	5	6
55	35.9	-	16.7	14.7	8.4	1.1
50	33.6	17.5	16.0	12.6	7.1	.7
45	32.9	11.4	8.7	9.4	4.4	.7
40	29.1	7.7	5.7	6.3	2.1	.4
35	61.2	12.1	10.3	6.2	2.8	.4
30	66.7	11.5	7.6	5.8	1.8	.4

Table 35. B_i Values used to calculate both the zonal and meridional components of eddy diffusivity.

Alt	Season			
	Winter	Spring	Summer	Fall
55	.12	.33	.33	.08
50	.12	.33	.33	.08
45	.19	.33	.33	.09
40	.25	.33	.33	.09
35	.41	.33	.33	.21
30	.56	.33	.33	.33

SUMMARY AND CONCLUSIONS

In most instances, the zonal component of eddy diffusivity is three to five times as large as its meridional counterpart. Both vary greatly with season, latitude, and altitude. Largest magnitudes are found in the vicinity of 38°N at 35 km, while eddy diffusivities within the easterlies, even in regions of relatively strong flow, average one order of magnitude less. In the tropics, where seasonal variations in the wind field are much smaller, both components of eddy diffusivity remain relatively constant throughout the year. Maximum annual stratospheric values of the zonal diffusivity component occur near 40°N at 35 km, while maximum annual stratospheric meridional values occur near 60°N at 30 km. Both zonal and meridional diffusivity components have annual tropopausal maximums, the zonal maximum occurring at 40°N, while the meridional maximum occurs at 50°N. Annually, a diffusivity minimum is located between 20 and 25 km for both diffusivity components.

Unfortunately, dispersion rates in the region of SST travel are, therefore, rather small in comparison with the troposphere and upper stratosphere. Assuming that the vertical component of eddy diffusivity is proportional to horizontal diffusivities, convergence would be present in the lower stratosphere due to the higher vertical diffusivities above and below. Mixing between the troposphere and upper stratosphere should also be rather slow.

Striking similarities between the variance and eddy diffusivity analyses demonstrates that variations in the intensities of the turbulent fluctuations are chiefly responsible for the strong seasonal, latitudinal, and altitudinal dependence. Although wave dynamics are not well understood above 30 km, part of these fluctuations may be explained by traveling planetary waves of two-week periods found in the winter by Hirota (1968) and during summer by Meunch (1969) and Hirota (1975). Part of the greater winter variance can be attributed to stratospheric sudden warmings, both major and minor. Fluctuations on a smaller scale may be produced by interactions between vertically-propagating waves and

strong westerly flow (Wofsy and McElroy, 1973). In any case, a better understanding of stratospheric dynamics is necessary in order to more thoroughly explain the variations in eddy diffusivity.

ACKNOWLEDGMENTS

The authors wish to thank F. J. Schmidlin for his many valuable discussions and assistance. This research is sponsored by the National Aeronautics and Space Administration, Contract NAS 6-2498.

REFERENCES

Belmont, A. D., Dartt, D. G., and Nastrom, G. D.: Periodic variations in stratospheric zonal wind from 20 to 65 km, at 80°N to 70°N. Quart. J. Roy. Meteor. Soc., 100, 203-211, 1974.

Charney, J. G., and Drazin, P. G.: Propagation of planetary-scale disturbances from the lower into the upper atmosphere. J. Geophys. Res., 66, 83-109, 1961.

Hay, J. S. and Pasquill, F.: Adv. Geophys. Vol. VI. Academic Press, 345 pp, 1969.

Hirota, I.: Planetary waves in the upper atmosphere in early 1966. J. Meteor. Soc. Japan, 46, 418-430, 1968.

_____ : Spectral analysis of planetary waves in the summer stratosphere and mesosphere. J. Meteor. Soc. Japan, 53, 34-44, 1975.

Kao, S. K.: Some aspects of large-scale diffusion and turbulence in the atmosphere. Quart. J. Roy. Meteor. Soc., 91, 10-19, 1965.

_____, and Bullock, W. S.: Lagrangian and Eulerian correlations and energy spectra of geostrophic velocities. Quart. J. Roy. Meteor. Soc., 94, 40-62, 1964.

_____, and al-Gain, A. A.: Large-scale dispersion of clusters in the atmosphere. J. Atmos. Sci., 25, 214-221, 1968.

_____, and Powell, D. C.: Large-scale dispersion of clusters in the atmosphere II. stratosphere. J. Atmos. Sci., 26, 734-740, 1969.

Murgatroyd, R. J.: Estimations from geostrophic trajectories of horizontal diffusivity in the mid-latitude troposphere and lower stratosphere. Quart. J. Roy. Meteor. Soc., 94, 40-62, 1969.

Neuch, H. S.: Large-scale disturbances in the summertime stratosphere. J. Atmos. Sci., 25, 1108-1115, 1968.

Newell, R. E. et al.: The General Circulation of the Tropical Atmosphere and Interactions with Extratropical Latitudes. Vol. I, MIT Press, 252 pp, 1972.

Reed, R. J. and German, K. E.: A contribution to the problems of stratospheric diffusion by large scale mixing. Mon. Weather Rev., 93, 313-321, 1965.

Taylor, G. I.: Diffusion by continuous movements. Proc. London Math. Soc., Ser. 2, 20, 196-211, 1921.

Wofsy, S. C. and McElroy, M. B.: On vertical mixing in the upper stratosphere and lower mesosphere. J. Geophys. Res., 78, 2619-2624, 1973.

1. Report No. NASA CR-3006	2. Government Accession No.	3. Recipient's Catalog No.
4. Title and Subtitle HORIZONTAL EDDY DIFFUSIVITIES IN THE NORTHERN HEMISPHERIC STRATOSPHERE AND LOWER MESOSPHERE		5. Report Date June 1978 6. Performing Organization Code
7. Author(s) S. K. Kao, R. J. Okrasinski and N. J. Lordi		8. Performing Organization Report No. 10. Work Unit No.
9. Performing Organization Name and Address Department of Meteorology University of Utah Salt Lake City, Utah 84112		11. Contract or Grant No. NAS6-2498 13. Type of Report and Period Covered Contractor Report
12. Sponsoring Agency Name and Address National Aeronautics and Space Administration Wallops Flight Center Wallops Island, Virginia 23337		14. Sponsoring Agency Code
15. Supplementary Notes		

16. Abstract

Meteorological rocket soundings, launched between 1969-74 at six locations representative of low, middle, and high altitudes, are employed with the use of the statistical theory of diffusion, to determine the zonal and meridional component of eddy diffusivity between 30 and 55 km as a function of season, latitude, and altitude. A comparison is also made between annually-averaged eddy diffusivities above and below 30 km.

It is shown that the zonal component of eddy diffusivity is approximately three to five times as large as the meridional component, in most cases. Both components of eddy diffusivity vary greatly with season, latitude, and altitude. It is found that highest eddy diffusivities occur in the vicinity of the winter westerly jet located near the tropopause (Z=12 km, 40°N) and in the stratosphere at 35 km, 40°N. Annually, a minimum of the eddy diffusivity occurs near 20 km. In most cases, the zonal component of the eddy diffusivity is approximately three to five times as large as the meridional component. The meridional cross-section of the zonal and meridional components of the eddy diffusivity in the northern hemisphere are presented.

17. Key Words (Suggested by Author(s))	18. Distribution Statement
Meteorology Meteorological Rockets Turbulent Diffusion Stratosphere Environment Models	UNCLASSIFIED - Unlimited STAR Category 47

19. Security Classif. (of this report)	20. Security Classif. (of this page)	21. No. of Pages	22. Price*
Unclassified	Unclassified	75	$5.25

* For sale by the National Technical Information Service, Springfield, Virginia 22161

NASA-Langley, 1978

END

9. 19. 78